Unequal scaling of urban vegetation cooling across sociodemographic groups

Yuyang Chang [1*], Gabriele Manoli [2], Alby D. Rocha [3], Jonas Schwaab [4], Maarten J. van Strien[5], Dominic A. Martin [6], Ronita Bardhan [7], Jaboury Ghazoul [1], Fritz Kleinschroth [4*]

1 Ecosystem Management, Department of Environmental Systems Sciences, ETH Zurich, Zurich, Switzerland

2 Laboratory of Urban and Environmental Systems, École Polytechnique Fédérale de Lausanne, Lausanne, Switzerland

3 Earth Observation and Geoinformatics Division, INPE - National Institute for Space Research, São José dos Campos - SP, Brazil

4 Institute for Environmental Planning, Leibniz Universität Hannover, Hannover, Germany

5 Planning of Landscape and Urban Systems, Department of Civil, Environmental and Geomatic Engineering, ETH Zurich, Zurich, Switzerland

6 Department of Environmental Sciences, Wageningen University, Wageningen, Netherlands

7 Sustainable Design Group, Department of Architecture, University of Cambridge, Cambridge, United Kingdom

Corresponding authors*

Yuyang Chang, email: yuyangchang.yc@gmail.com

Fritz Kleinschroth, email: kleinschroth@umwelt.uni-hannover.de

*This paper is a **non-peer reviewed** preprint submitted to EarthArXiv.*

Abstract

Urban vegetation cools cities, but its benefits often reach disadvantaged residents least, a growing concern as urban heat risks intensify. Whether residence-based cooling exposure and its inequality scale systematically with population size and density, as infrastructural and socioeconomic attributes do, remains unclear. Here, we simulate vegetation cooling across Switzerland using process-based modeling and link estimates to geocoded census records for over seven million urban residents. Mean cooling per resident decreases in denser and more populous areas, with steeper declines among socioeconomically disadvantaged residents and temporary-permit holders. Cooling inequality rises with population size and density, and over a third of Swiss municipalities combine above-average inequality with benefits favoring socioeconomically advantaged or permanently settled residents. By classifying both the magnitude and social direction of inequality across municipalities and 1-km² cells, we provide a spatial diagnostic for equitable, climate-resilient greening interventions. Our findings reveal vegetation-cooling inequality as an emergent scaling property of cities.

Main

Urban vegetation is a frontline tool for climate adaptation, providing canopy shade and evapotranspirative cooling that reduce heat exposure and improve well-being in urban areas[1,2]. Yet the burden of urban heat is unequally distributed: low-income and minority communities generally face higher ambient temperatures and fewer adaptive resources[3,4]. Urban vegetation access is itself heterogeneously stratified[5]: socially disadvantaged residents tend to live in areas with less green cover, with fewer heat adaptation options[6,7]. As urban heat risks are projected to intensify under climate change[8], ensuring equitable distribution of vegetation cooling benefits has become a key challenge for climate-resilient cities.

Even within the same urban area, residents may receive markedly different vegetation-cooling benefits around their homes, and these differences may align systematically with socioeconomic and demographic characteristics. Assessing such distributive equity requires fine-resolution climate and vegetation data linked to geocoded demographic information, three data streams that are rarely combined at national scale in a single analysis. Most assessments of urban vegetation cooling rely on satellite-based proxies such as NDVI or land surface temperature[9,10], which capture broad spatial patterns but are indirect measures of actual microclimatic conditions[11]. Field-based sensor campaigns provide more direct observations, showing, for instance, that tree canopies deliver substantially stronger cooling than short-statured vegetation[12,13], but remain spatially sparse and are rarely linked to demographic information. Process-based models, such as ENVI-met [14], simulate canopy shading and evapotranspiration more accurately, but their high computational demands at the neighborhood scale have limited their use for national-scale assessment of distributive justice in vegetation-cooling benefits. On the demographic side, socioeconomic data are generally available only at coarse administrative units[15,16]. Unpopulated zones within large administrative boundaries inflate the apparent cooling available to residents, and aggregation effects can obscure within-neighborhood contrasts and misrepresent individual exposure[17]. Furthermore, administrative-unit-level data cannot accurately capture residents' immediate cooling environments across different radii around their homes[18]. Geo-coded individual-level microdata would enable direct linkage of residential location to cooling environment, but privacy constraints make such data rarely available at population scale[19]. These constraints have prevented individual-level assessment of vegetation cooling equity across social groups at national scale.

Yet precise individual-level measurements alone cannot reveal whether cooling patterns generalize across cities of different sizes. Guiding equitable cooling interventions across urban size and density scales requires understanding how per-resident vegetation cooling is systematically distributed along the population gradient and whether this varies across social groups. Urban scaling laws provide a generalized framework for such complex distributional challenges[20]. Originally developed to describe how city-level properties vary systematically with total city population, scaling analysis has revealed that cities follow consistent regularities regardless of their cultural and geographic context[21]. Socioeconomic properties such as GDP, innovation, and crime scale superlinearly, which means larger cities produce disproportionately more per capita[22,23], while physical infrastructures such as public facilities scale sublinearly, reflecting efficiency gains[24]. These regularities have since been extended to urban environmental outcomes, including waste generation[25] and air pollution[26]. Urban scaling laws have also been applied to test the within-city and across-city urban inequality distributions of human networking, productivity, and infrastructure[27,28]. Most recently, scaling has been applied to urban climate, showing that intra-urban temperature variability follows general scaling functions across cities worldwide[29]. However, if vegetation cooling as an urban temperature regulation tool conforms to such a scaling relationship, and if these patterns differ across social groups, remains unknown.

Europe has experienced increasingly frequent and severe heat events in recent decades, with heat-related mortality rising across the continent[30,31]. Within this warming context, Switzerland, warming at approximately 1.6 times the northern hemispheric average rate[32], presents a particularly timely setting for examining cooling equity, offering a richly diverse sociodemographic profile alongside exceptional individual-level data availability. Foreign nationals account for 27.7% of the permanent resident population, 19.8% are aged 65 or older, and 6.0% are aged 80 or older[33], a composition that naturally stratifies heat vulnerability across multiple demographic dimensions[34]. Evidence from other countries suggests that residents with lower heat-adaptation capacity seek nature-based cooling solutions[35]. In Switzerland, where fewer than 10% of households are air-conditioned [36] and urban green space access is highly unequal[37], the distribution of vegetation cooling benefits is particularly consequential. Yet whether vegetation cooling reaches the most vulnerable residents, or compounds existing disparities, and how these patterns scale across population size and density, remain open questions.

Here, we use the process-based Soil Canopy Observation of Photosynthesis and Energy fluxes (SCOPE) model[38] to estimate vegetation cooling across Switzerland at 10 m resolution and link these estimates to geo-coded census records for more than seven million urban residents, yielding residence-based cooling exposure for each individual. We characterize how cooling exposure varies across five sociodemographic indicators, residence permit type, civil status, age, gender and socioeconomic position, and across spatial extents of 20-1,000 m around each residence. We then test whether mean per-resident cooling declines with population size and density, and whether this scaling differs by socioeconomic position and residence permit status. Finally, we apply a joint Gini-Concentration Index framework at both municipal and 1 km² cell levels to identify locations where cooling benefits are both highly unequal and disproportionately concentrated among advantaged groups, providing a dual diagnostic for equitable greening interventions. This work tests whether vegetation cooling follows systematic scaling relationships with population size and density, and whether inequality in its distribution emerges as a scaling property of cities.

Results

Geography of vegetation cooling across Switzerland

Cooling benefits from urban vegetation exhibited strong spatial heterogeneity across Switzerland (Fig. 1a). Cooling benefits are quantified using the Greening Cooling Services (GCoS) index, a unitless 0-1 metric integrating vegetation's radiative and evapotranspirative cooling at 10 m resolution, derived from an hourly process-based simulation (SCOPE model; see Methods), representing the maximum potential cooling supply under peak summer heat conditions. Population-weighted cooling benefits and background air temperatures vary across biogeographical regions and cantons. Background air temperature is defined as the mean air temperature (Ta mean) at 100 m resolution on the most extreme summer heat day, representing the most severe thermal exposure conditions for populated areas. At the cantonal level, background temperatures vary widely, while average cooling values show a narrower range because the GCoS is a bounded index (Fig. 1b). Cantons that experience high background temperatures (> 26 °C) while still receiving relatively high cantonal-average cooling benefits include Zurich and Basel-Landschaft; the densely built canton of Basel-Stadt, by contrast, combines comparably high temperatures with markedly lower cooling. Cantons like Valais and Jura display the lowest average cooling benefits.

The population's exposure to these cooling benefits is unevenly distributed relative to background heat (Fig. 1c). The vast majority of Swiss residents are concentrated in areas experiencing high mean summer air temperatures, with population exposure peaking strongly near 27 °C. In contrast, the population is disproportionately exposed to only moderate levels of vegetation-induced cooling (peaking between 0.4 and 0.5), with a negligible fraction of residents experiencing high cooling benefits (> 0.7). This uneven demographic exposure is further reflected across biogeographical regions (Fig. 1d). Population-weighted median cooling benefits are highest in the Central Plateau and Jura regions, where background temperatures are also the most severe.

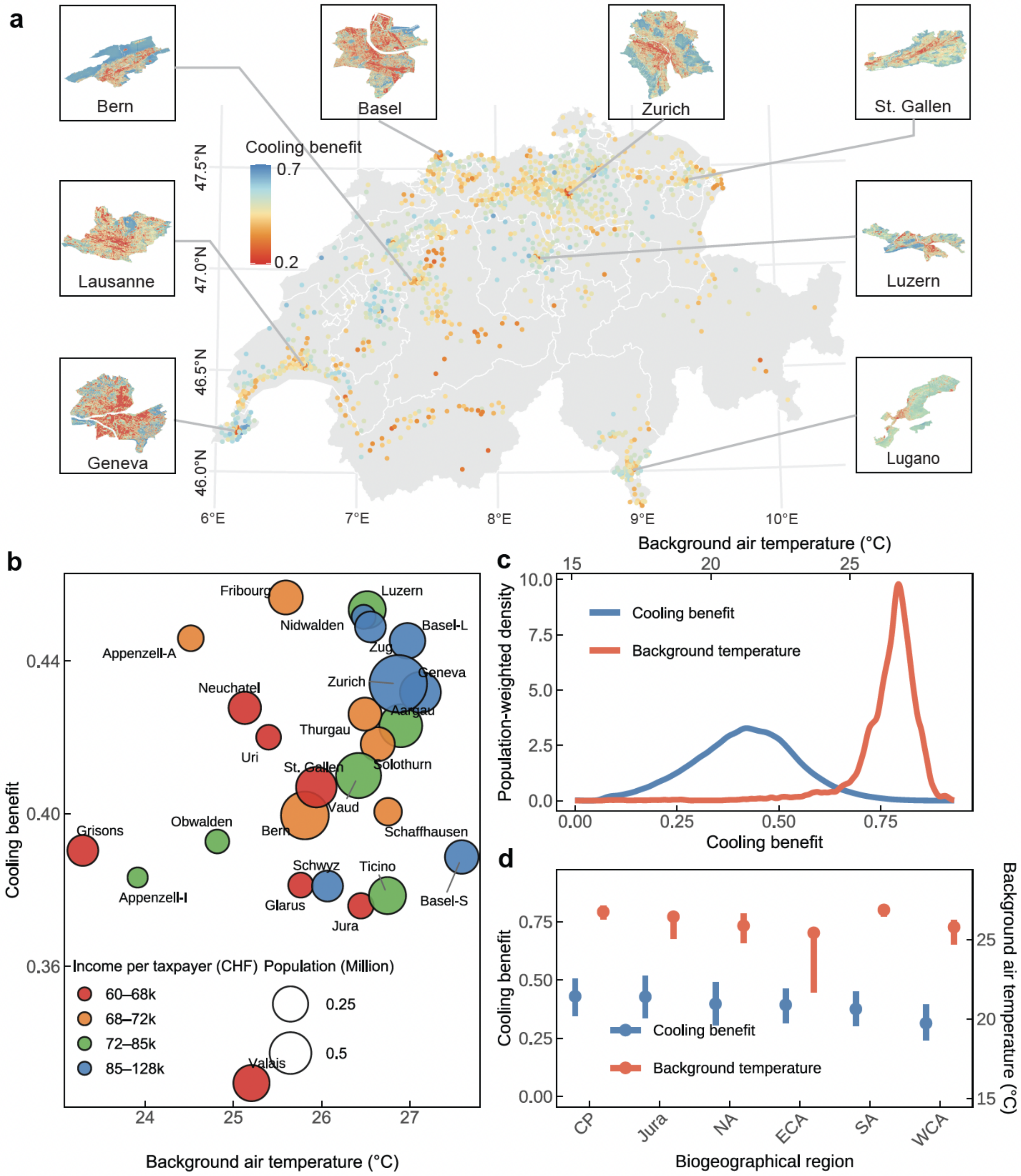

Fig. 1. Geographic and demographic distribution of cooling benefits from urban vegetation across Switzerland. a, Spatial distribution of the cooling benefit (quantified as the unitless Greening Cooling Services index, GCoS) averaged at the municipal level (excluding rural municipalities). Insets highlight the spatial cooling patterns within eight major Swiss cities. b, Cantonal-level relationship between population-weighted average cooling benefits, background air temperatures, and socioeconomic characteristics. Bubble size corresponds to the cantonal population (in millions), while color denotes the median income per

taxpayer (CHF). c, Population-weighted density distributions of cooling benefits (blue line, bottom x-axis) and background air temperatures (red line, top x-axis). Background temperature represents the mean air temperature (Ta mean). d, Population-weighted median cooling benefits (blue, left y-axis) and background temperatures (red, right y-axis) across six biogeographical regions of Switzerland. Vertical bars represent the population-weighted interquartile range (25th-75th percentile). Biogeographical regions include the Jura, Central Plateau (CP), Northern Alpine Slope (NA), Southern Alpine Slope (SA), Eastern Central Alps (ECA), and Western Central Alps (WCA). Municipality and biogeographic region classifications are shown in Fig. S1. All analyses are based on 2018, a warm but not extreme summer year that slightly exceeded the upper bound of the ±1 standard deviation range around the 1990-2024 long-term mean Swiss summer temperature (Fig. S2).

Cooling benefits from urban vegetation across social groups and distance

We quantify disparities of cooling benefits at residential addresses (1 m resolution) for over 7 million Swiss residents, extracting mean cooling benefits within buffers from 20 to 1000 m at 20 m intervals around each address. We assess cooling benefits across five sociodemographic indicators: age, residence permit type, socioeconomic position (SEP), gender, and civil status. We excluded nationality from the main analysis due to high correlation with residence permit type (Fig. S3).

We report cooling medians at a focal radius of 100 m (Fig. 2a), the buffer radius at which measured cooling stabilizes (r_{95}; Fig. 2b), and how median cooling varies across buffer radii from 20 to 1000 m (Fig. 2c); the observed medians and interquartile ranges at each radius, from which those lines are fitted, are shown in Fig. S4. Cooling magnitude varies significantly across all five indicators (Fig. 2a; pairwise bootstrap statistics in Table S1). Disparities are largest for residence permit type and SEP: cooling is highest among Swiss citizens and lowest among short-term (L permit) holders, with the SEP gradient strictly ordered from high to low. Age, gender, and civil status differences are statistically significant but smaller in magnitude. These patterns hold after controlling for all five indicators simultaneously, with permit type and SEP retaining the largest independent cooling deficits in a multiple linear regression (Fig. S5). The one exception is the youngest group (0-25): their unadjusted median cooling is lower than that of 65-79-year-olds, whereas their adjusted mean coefficient is positive. This suggests that the apparent deficit of the youngest group is not independent of their socioeconomic and residential characteristics. Sociodemographic rank orderings are consistent across the full 20-1000 m range (Fig. 2c), with disparities present at the smallest scales measured and persisting across broader extents. Disadvantaged groups additionally require longer distances to reach their cooling saturation: short-term permit holders saturate at r_{95} = 167 m, compared to 82 m for Swiss citizens, and low-SEP residents at 100 m, compared to 65 m for high-SEP residents (Fig. 2b). These patterns persist within population density tertiles (Fig. S6), confirming they are not driven by residential density sorting.

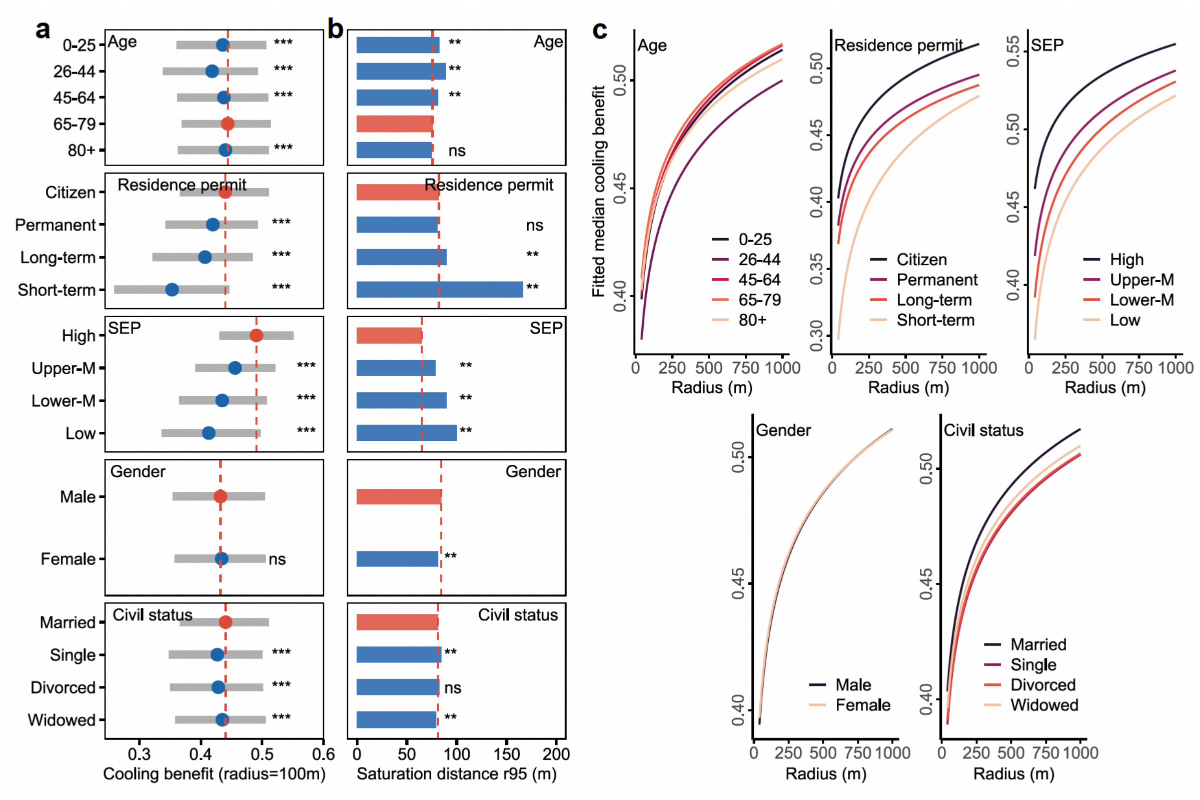

Fig. 2. Sociodemographic disparities in cooling benefits from urban vegetation. a, Median cooling benefit at a focal radius of 100 m, stratified by five sociodemographic indicators: age, residence permit type, socioeconomic position (SEP), gender, and civil status. Points indicate group medians; horizontal bars denote interquartile ranges (25^{th}-75^{th} percentiles), shown as a descriptive measure of spread; statistical inference is based on the resampling procedures described in Methods. Red denotes the reference group for each indicator and blue all other groups. The vertical dashed line marks the median value of the reference group for each indicator (shown in parentheses); bootstrap pairwise significance stars indicate tests versus that reference (*** $p < 0.001$, ** $p < 0.01$, ns not significant). b,

Saturation distance (r_{95}): the focal radius at which 95% of the fitted asymptotic cooling benefit is reached, by sociodemographic group. Bar length indicates the group r95 value, with color coding and dashed line as in a. Bootstrap standard errors are reported in Table S4. c, Log-linear relation between cooling benefit and focal radius (20-1000 m) by sociodemographic group; lines show fitted values; each sub-panel corresponds to one indicator. Residence permit categories: Citizen = Swiss citizens (passport holders); Permanent = permanent residence permit (C); Long-term = long-term work/study permit (B); Short-term = short-term permit (L).

Socially stratified urban scaling of cooling benefits

Urban scaling laws describe how city-level properties vary with population size as a power law, and a negative scaling exponent ($\beta < 0$) indicates that denser or larger urban areas provide lower per-capita levels of that property. Applying this framework, we test whether cooling benefits from urban vegetation scale with population, and whether the scaling exponent differs by social group, at two spatial levels: 1 km^2 cell (population density) and municipalities (population size). Cooling benefits are measured as the mean vegetation cooling within buffer radii from 100 to 1,000 m around each residential address, and results are reported across this range to confirm robustness.

Mean cooling benefits at a 100 m focal radius decline with population density ($\beta = -0.058$; Fig. 3a), indicating that denser areas provide weaker local cooling. Residents with the lowest cooling within each 1 km^2 cell (P10, the 10th percentile of the local cooling distribution; $\beta = -0.079$) show a steeper decline with population density than those with the highest (P90; $\beta = -0.044$; $\Delta\beta = +0.035$, $p < 0.001$), indicating that denser environments disproportionately disadvantage those already receiving the least cooling. For residence permit status, permanent residents show a shallower cooling decline than temporary permit holders, though the difference is small ($\Delta\beta = +0.004$; Fig. 3b). The SEP gradient is more pronounced: High-SEP residents show a shallower decline ($\beta = -0.042$) than low-SEP residents ($\beta = -0.068$; $\Delta\beta = +0.026$; Fig. 3c). These scaling patterns persist across all focal radii from 100 to 1,000 m, with all group gaps largest in the immediate residential environment and attenuating at broader extents (Fig. 3a-c insets).

When examining the relationship between mean cooling benefits and municipality population size, negative scaling persists but is weaker (β = -0.026; Fig. 3d-f), indicating that population size captures less of the cooling variation than population density. The P10-P90 gap widens (Δβ = +0.050); the permit gap, though small, is more pronounced than at the density level (Δβ = +0.010). These results confirm that the negative scaling of cooling benefits with population is universal, but its rate of attenuation is consistently steeper for socially disadvantaged residents.

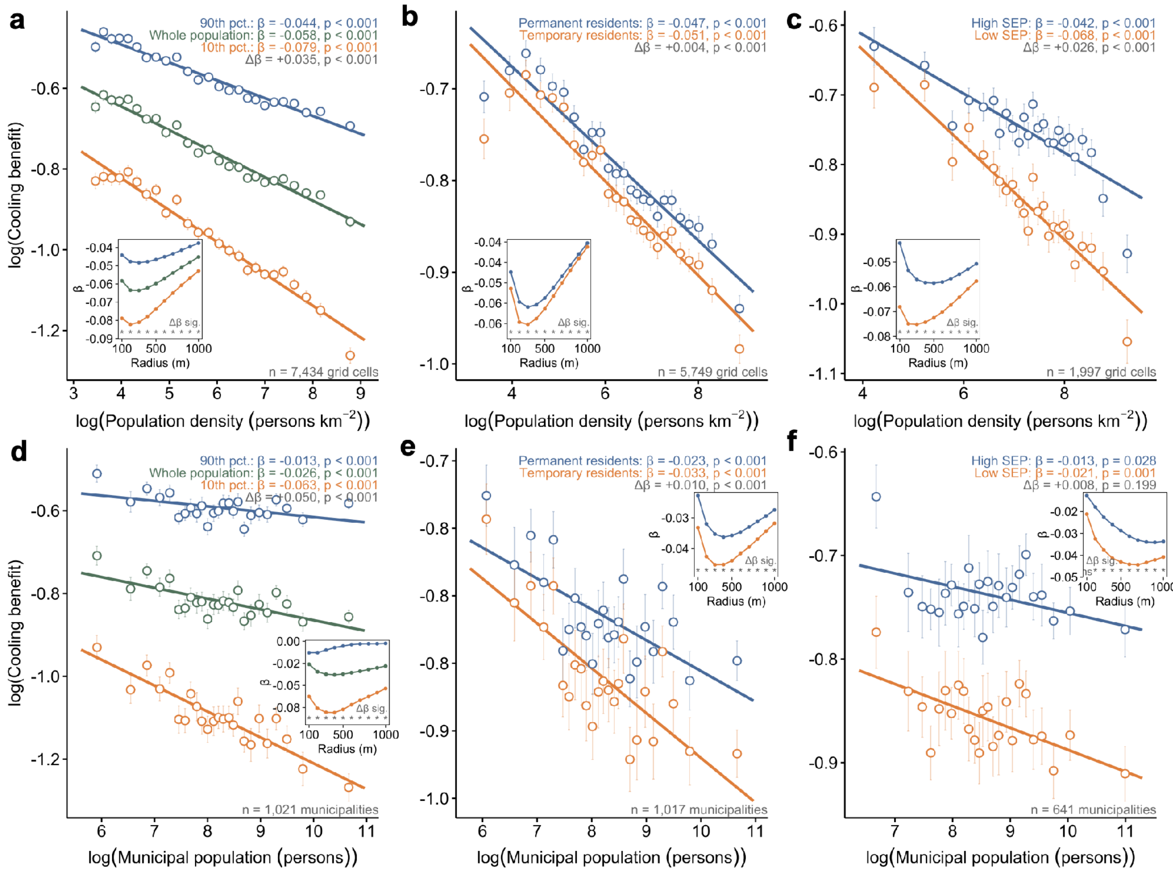

Fig. 3. Socially stratified urban scaling of cooling benefits from urban vegetation. Log-log scaling regressions of mean individual cooling benefits (100 m radius) against population density and size, stratified by social group. Points show means within 25 equal-count bins along the x-axis, with vertical bars giving the standard error of the mean in each bin; binning is for display only, and all regression lines and scaling exponents are fitted to the unbinned data. Panels a-c show results for 1 km² population density (persons km^{-2}); panels d-f show results for municipalities, where population is the total municipal population. a and d: scaling of the whole population (green), the 90th percentile (90th pct., blue; individuals with the highest cooling exposure within each unit), and the 10th percentile (10th pct., orange;

individuals with the lowest cooling exposure). b and e: permanent residents (Swiss citizens and holders of permanent residence permits (C); blue) and temporary residents (orange). c and f: in the top 25% (high SEP, blue) and bottom 25% (low SEP, red) of socio-economic position (SEP). Insets show scaling exponents estimated across focal radii from 100 to 1,000 m (100 m intervals); significance stars indicate a significant difference in scaling exponents between the two groups (see Methods; *p < 0.05, ns not significant).

Spatial distribution and scaling of cooling inequality

We examine cooling inequality using the Gini index mapped at both the 1 km^2 cell level and the municipality level (Fig. 4a-b). The Gini index scales positively with population size at both spatial scales: at a 100 m focal radius, the scaling exponent is $\beta = 0.126$ at the 1 km^2 level and $\beta = 0.083$ at the municipality level (both $p < 0.001$; Fig. 4c), indicating that cooling inequality is greater in more populated units. This positive scaling persists across all focal radii from 100 to 1,000 m, with both β and R^2 increasing gradually with focal radius, suggesting that inequality in cooling over broader neighborhoods is more tightly coupled to population size. Results are robust to the choice of inequality measure: an equivalent analysis using the Theil index, an entropy-based alternative to the Gini, yields the same scaling pattern (Fig. S7; Table S2).

We also compared Gini values between residence permit and SEP subgroups at the 1 km^2 cell level (Fig. 4d-e) and municipality level (Fig. S8). For residence permit groups, the Gini index for temporary and permanent residents is closely aligned (slope = 0.95, $R^2 = 0.60$ at 100 m focal radius), indicating similar magnitudes of within-group cooling inequality across residential status groups. For socioeconomic position (SEP), Gini values for residents in the bottom 50% SEP fall systematically below those of the top 50% SEP (slope = 0.43 at a 100 m focal radius; 0.59 at 1,000 m), suggesting that higher-SEP residents exhibit greater heterogeneity in cooling access, while the cooling environment of lower-SEP residents tends to be more homogeneous. The Theil index confirms the same within-group patterns (Fig. S7, d-e).

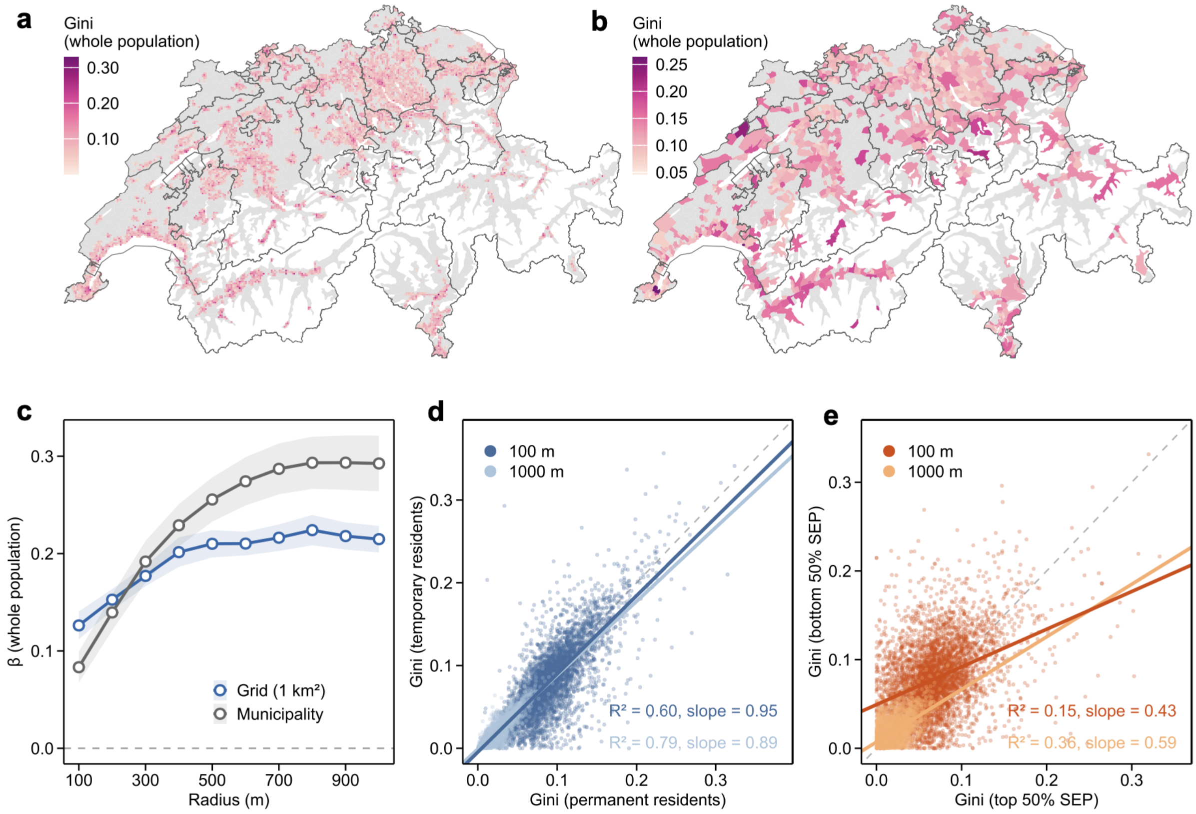

Fig. 4. Spatial distribution and urban scaling of cooling inequality. a-b, Spatial distribution of the Gini index of cooling inequality at (a) the 1 km² cell level and (b) the municipality level, computed at a 100 m focal radius; units with fewer than 20 residents are excluded; cantonal boundaries are shown in dark grey. c, Scaling exponent (β) of the Gini index against population size, estimated at the 1 km² cell (blue circles) and municipality (grey circles) levels across focal radii from 100 to 1,000 m (100 m steps); shaded ribbons show 95% confidence intervals. d-e, pairwise comparison of subgroup Gini values at the 1 km² cell level, shown at focal radii of 100 m (dark) and 1000 m (light), for (d) temporary versus permanent residents and (e) residents in the bottom 50% versus the top 50% of socioeconomic position (SEP). Dashed lines indicate the 1:1 equality line; solid lines show ordinary least squares regression fits with reported slope and R^2 values.

Cooling equity typology at municipal and 1 km² cell levels

To characterize how cooling inequality and its social distribution co-vary across local contexts, we jointly examine the Gini index and the Concentration Index (CI) in Gini-CI space across all Swiss municipalities (Fig. 5). Higher Gini values indicate greater internal inequality in cooling exposure; the CI captures the social direction of cooling, whether benefits disproportionately favor disadvantaged (negative CI) or advantaged (positive CI) residents. Municipalities show a positive Gini-CI association, indicating that higher cooling inequality typically coincides with cooling favoring socially advantaged populations. This holds for SEP and residence permit status (Fig. 5a, e). The same positive association is observed when focusing on elderly residents, comparing those aged 80+ against the 65-79 group (Fig. S9a).

The Gini-CI space yields four cooling equity typology quadrants defined by inequality level and who benefits from cooling. The largest share falls in the upper-right quadrant (36% for SEP; 40% for permit type), above-average inequality combined with pro-advantaged cooling, the least equitable configuration (e.g., Geneva for SEP, Zurich for permit type; Fig. 5c, g). A smaller share occupies the lower-left quadrant (13% for SEP; 12% for permit type), where cooling is more evenly distributed and modestly favors disadvantaged residents (e.g., Horgen for SEP, Riehen for permit type; Fig. 5d, h). Among elderly residents, 32% of municipalities show above-average cooling inequality concentrated among the 65-79 group, while 21% show below-average inequality with cooling modestly favoring the 80+ group (e.g., Lugano and Frauenfeld respectively; Fig. S9d-e). The full Gini-CI typology at the 1 km^2 cell level is mapped nationally (Fig. S10), extending this classification to individual neighborhoods and providing a granular basis for spatially targeted greening interventions.

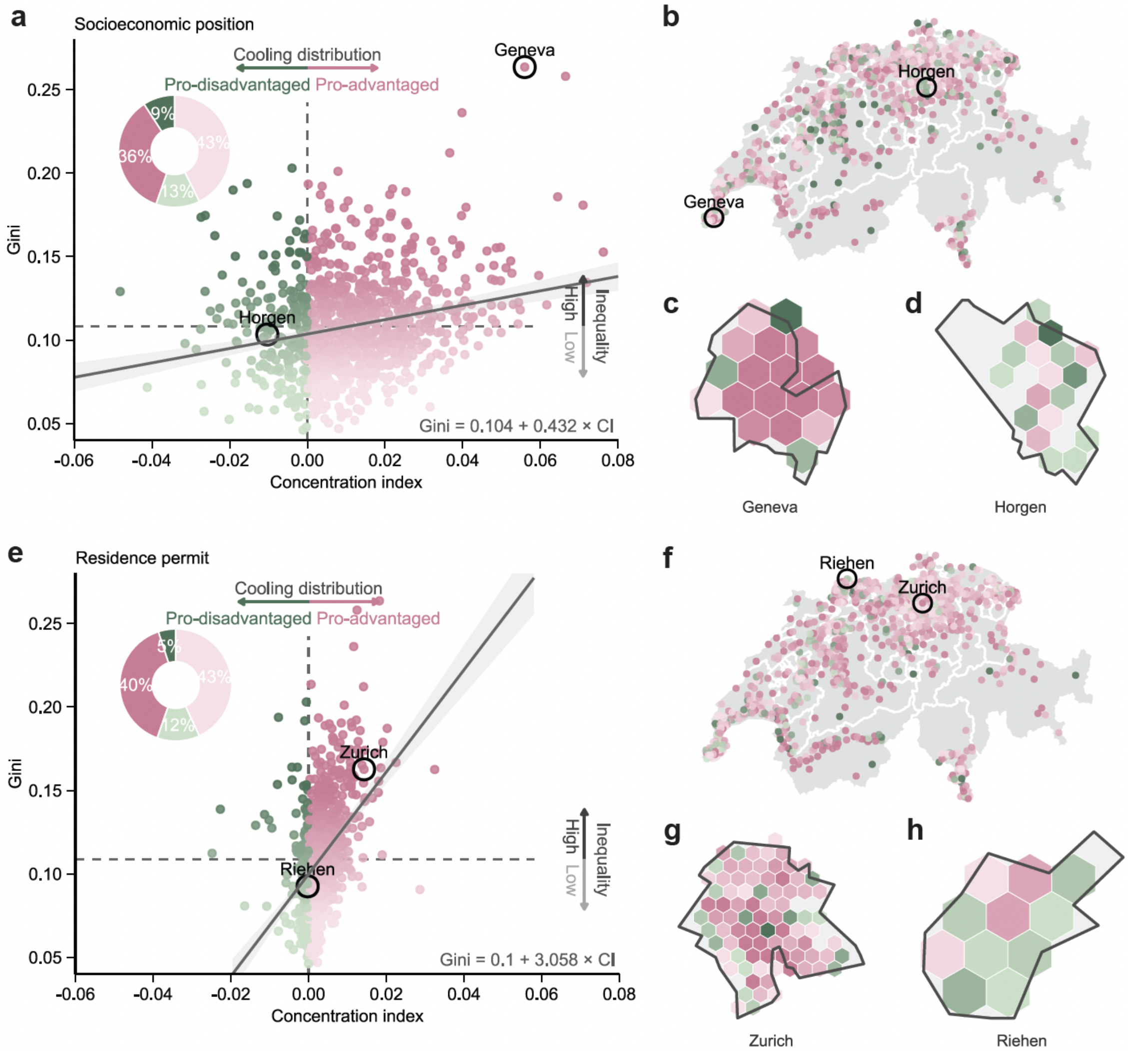

Fig. 5. Municipal-level cooling inequality and equity typology for socioeconomic position (SEP) and residence permit type. a, e, Each point represents one municipality in Gini-CI space; the Gini index (y-axis) measures internal inequality in cooling exposure derived from individual-level 100 m focal cooling, and the Concentration Index (CI; x-axis) captures the social direction of cooling, negative CI indicates cooling concentrated among disadvantaged residents, positive CI indicates cooling concentrated among advantaged residents. Dashed lines mark the mean Gini (horizontal) and CI = 0 (vertical), dividing municipalities into four quadrants; in the figure, "high" and "low" inequality refer to Gini values above and below this cross-municipality mean, corresponding to above- and below-average inequality in the main text; insets show the percentage of municipalities in each quadrant. Regression lines show fitted linear relationships with 95% confidence intervals. b, f, Geographic distribution of municipalities colored by Gini-CI quadrant; pink indicates the upper-right quadrant

(above-average inequality, pro-advantaged) and green indicates the lower-left quadrant (below-average inequality, pro-disadvantaged); annotated examples illustrate contrasting profiles. c-d, g-h, Within-municipality cooling patterns at the 1 km² cell level for selected contrasting municipalities, illustrating the least equitable (c, g) and more equitable (d, h) profiles for SEP and permit type, respectively.

Discussion

Our results show that with increasing concentration of people, cities provide shrinking per-resident vegetation cooling, and they do so unequally. By applying inequality indices at fine spatial resolution we reveal where cooling is most unequally distributed and who bears heat burdens, providing a diagnostic foundation for targeted equitable greening interventions.

Vegetation cooling supply is systematically lower in more populous areas, following a negative power-law relationship with population density. This is consistent with evidence that per-capita green space access declines with city size[39], and provides a complementary biophysical interpretation: vegetation's contribution to cooling shrinks as urban areas concentrate more residents. While this negative association is somewhat intuitive, our results situate it within the broader framework of urban scaling laws. Crucially, $\beta < 0$ represents an absolute per-resident cooling deficit that deepens with population density, a qualitatively different regime from the agglomeration benefits that characterize physical infrastructure and public services, which typically scale positively with population size[40,41]. The cooling pattern likely reflects the declining ratio of vegetated surface to residents with increasing density[42,43], as well as the constrained growing conditions that limit the biophysical capacity of urban vegetation in compact environments[44,45]. Our results therefore suggest that the logic of urban agglomeration efficiency does not readily translate to climate regulation services from vegetation[46,47], suggesting that climate regulation services from vegetation obey their own distinct scaling regime, potentially governed by constraints of land surface, radiative balance, and vegetation function[48].

The SCOPE model has also been applied for measuring green cooling across major European cities, where unprivileged groups were found to receive less green cooling[49]. That work characterizes disparities within individual cities; by resolving cooling at the level of individual residents across an entire national urban system, we can additionally test how those disparities scale with population size and density. Cooling benefits decline steeply with population density and municipality size for socioeconomically disadvantaged residents, indicating that the cooling penalty of density is not socially neutral, consistent with documented green space access disparities in cities[7]. Residents in the High SEP distribution experience a shallower cooling decline (β = -0.042) than those in the Low-SEP group (β = -0.068), a gap of Δβ = +0.026, while the gap by permit status is comparatively modest (Δβ = +0.004). Therefore, socioeconomically disadvantaged residents experience steeper cooling loss in denser areas, widening the gap precisely where lower-SEP populations are disproportionately concentrated[50]. This double penalty is compounded by a structural feature visible in the within-group Gini comparison (Fig. 4d-e): lower-SEP residents and non-permanent permit holders show not only lower mean cooling (Fig. 2), but also lower within-group inequality, indicating that their cooling deprivation is pervasive across the group rather than concentrated among a subset. Denser and larger urban contexts amplify this universal inequality further[51].

Cooling inequality itself scales positively with population, meaning that larger and denser areas not only provide less mean cooling but distribute it more unequally. The Gini-CI (Concentration Index) typology, which has been applied in urban heat disparities research, sharpens these patterns into an actionable diagnostic[52]. The largest single group of Swiss municipalities falls in the above-average-inequality, pro-advantaged quadrant of Gini-CI space (36% for SEP, 40% for permit status), meaning cooling is both unequally distributed and disproportionately concentrated among socially advantaged residents. This reveals that equality of greening is insufficient: cooling equity requires that those who most need cooling have the greatest access to it[53], which demands interventions proportionate to cooling need, for example, highly heat-vulnerable oldest-old adults (aged 80 and above), and ecological deficit rather than uniform vegetation distribution[54–56]. The Gini-CI framework provides precisely the geographic targeting information required to act, identifying where inequality is most pronounced and socially asymmetric.

Although this study advances understanding of how urban vegetation cooling benefits scale with density and vary across sociodemographic groups, several limitations warrant consideration. First, the green cooling benefit index (GCoS) captures the maximum potential cooling supply from vegetation under peak heat conditions, derived from the SCOPE radiative and evapotranspirative model[57]; it does not account for the full urban energy balance, including building shading, albedo, and nocturnal dynamics[48], a constraint inherent to the computational demands of a national-scale simulation. Second, Swiss cities are small by international standards, so the scaling relationships reported here are estimated over a comparatively narrow range of urban population sizes and should be extrapolated to large metropolitan systems with caution. Furthermore, exposure is measured at the place of residence and does not account for daily mobility; cooling experienced at workplaces, schools or during travel is not captured.

Methods

Data

Meteorological data. Hourly meteorological variables were obtained from the ERA5 reanalysis dataset of the European Centre for Medium-Range Weather Forecasts (ECMWF), accessed via the Copernicus Climate Change Service (C3S) [58]. The dataset includes air temperature (2 m), relative humidity, surface pressure, 10 m wind speed, and downwelling shortwave and longwave radiation. These hourly fields provided boundary conditions for the vegetation cooling model. Background air temperature was characterized using predicted daily high-resolution air temperature data (100 m × 100 m) for Switzerland by Flückiger et al. [59]

Terrestrial surface data. Vegetation structure and land surface parameters were extracted from multiple satellite and national sources. The Leaf Area Index (LAI) (300 m resolution) was obtained from the Copernicus Global Land Service [60]. Canopy height data (1 m resolution, 2020) were provided by the Swiss National Forest Inventory. Land cover and fractional vegetation surfaces were derived from the Swiss Habitat Map[61], which also provided delineations of inland water bodies (features < 0.1 km² excluded). Cultivated and agricultural surfaces were excluded from the fractional canopy cover calculation. Tree canopy cover at 10 m resolution was defined by applying a 1 m minimum height threshold to the Vegetation Height Model, isolating woody from herbaceous cover.

Demographic data. Person-level geo-coded demographic data (STATPOP; one record per resident, with residential coordinates at 1 m precision) were obtained from the Swiss Federal Statistical Office (STATPOP 2018), comprising age, gender, marital status, nationality, and residence permit type for all residents [62]. Because the individual-level income data is highly confidential in Switzerland, we use a micro-neighborhoods index, Socioeconomic position (SEP) to reflect the relative economic position. The SEP was derived from the Swiss Neighborhood Index of Socioeconomic Position (Swiss-SEP 2015), an area-based deprivation indicator defined for 1.54 million micro-neighborhoods, each centered on a residential building and comprising the 50 nearest households by road-network distance. The index combines median rent, educational attainment, occupational class, and household crowding via principal component analysis, standardized to 0-100 [63]. SEP was assigned to each individual via nearest-neighbor spatial join in EPSG:2056 coordinates and categorized into national quartiles. All data were accessed under a data-sharing agreement with the Swiss Federal Statistical Office and handled in compliance with Swiss data-protection regulations. Municipalities classified as rural ("ländlich") according to the Swiss Municipal Typology [64] were excluded to focus on urban and peri-urban areas, yielding a total analytical population of 7,358,605 residents in 1,165,052 micro-neighborhoods.

Reference year. All analyses use 2018 as the reference year. STATPOP 2018 was the most recent release available when the study was designed, and 2018 was also a warm but not extreme Swiss summer, slightly exceeding the upper bound of the ±1 s.d. range around the 1990-2024 long-term mean (Fig. S2). Using the same year for the demographic and meteorological inputs ensures that the population distribution and the modelled cooling supply refer to the same period. Canopy height (2020) and Swiss-SEP (2015) were the nearest available releases; both describe attributes that change slowly relative to the study period.

Modeling of urban green cooling supply

Cooling benefits were quantified using the Greening Cooling Services Index (GCoS), which integrates evapotranspirative (ECoS) and radiative (RCoS) components. In this study, we used the GCoS approach that was first established for Berlin [57] and then applied to many European cities [49]. The ET component was independently validated in a Swiss urban context (Basel) using eddy covariance tower measurements, achieving R^2 = 0.85-0.89 across two tower sites (obs = 1,652-1,697 half-hourly measurements per site, 2019/2021). GCoS is derived from the SCOPE (Soil Canopy Observation, Photosynthesis and Energy fluxes) model, a process-based approach that simulates canopy radiative transfer, heat fluxes, and energy balance [65]. Leaf area index and canopy height (see Terrestrial surface data) entered SCOPE as pixel-level inputs, driving the evapotranspirative and radiative components respectively; fractional canopy cover, computed as the proportion of 1 m sub-pixels exceeding the 1 m height threshold within each 10 m cell, was applied in the second modelling stage to scale simulated fluxes to the vegetated proportion of each cell. GCoS represents the combined relative cooling potential of vegetation, expressed as a unitless index (0-1) standardized to a 24-hour mean for each 10 m pixel. As a bounded relative index, GCoS captures the spatial pattern of vegetation cooling supply rather than absolute air-temperature reduction.

Because of Switzerland's substantial topographic variation, the hottest day in 2018 was identified independently for each canton based on daily mean air temperature, and the corresponding date's meteorological data were used as model input to calculate GCoS for that canton (Table S3). Following the parameterization of ref.[49], stomatal conductance and soil moisture parameters were held constant in space and time at their default values, and irrigation was not represented. GCoS therefore represents potential cooling supply under non-water-limited conditions and may overestimate realized cooling where vegetation experiences soil-moisture stress. Because these parameters are spatially uniform, they shift the absolute level of GCoS but not its relative spatial distribution, on which all comparisons reported here are based.

Multi-scale extraction of cooling exposure

Cooling benefits accessible to each resident were extracted using a moving-window approach at multiple spatial extents. For each resident, cooling benefits (GCoS values) were extracted at the residential address and averaged within circular buffers from 20 m to 1,000 m in 20 m steps (50 radii), capturing cooling at both immediate residential and broader neighborhood scales. Cooling values were subsequently aggregated to 1 km^2 cells, municipalities, cantons, and biogeographic regions for multi-scalar analyses.

Classification of sociodemographic groups

Sociodemographic indicators were classified as follows: (1) Age: 0-25, 26-44, 45-64, 65-79, and 80+ years; (2) Residence permit: four groups reflecting legal residency status: Swiss citizens, permanent residents (C permit), long-term residents (B permit, residence permit for work and study more than 1 year), and short-term residents (L permit, short-term less than 1 year); (3) Gender: male and female; (4) Civil status: married, single, divorced, and widowed; (5) SEP: four groups derived by categorizing the continuous Swiss-SEP score (0-100) into national quartiles: Low (Q1), Lower-Middle (Q2), Upper-Middle (Q3), and High (Q4). Nationality was additionally classified as Swiss citizen, EU/EFTA national, or non-EU/EFTA national. We computed pairwise Spearman rank correlations across all indicator-group combinations at the individual level (Fig. S3). The nationality was excluded from the main analysis owing to high correlation with residence permit type. Group definitions differ between the two analyses in the socioeconomic dimension by design. The scaling analysis

(Fig. 3) contrasts the extremes of the SEP distribution, high (Q4) versus low (Q1), to characterize the steepest social gradient in cooling supply. For between-group comparisons of inequality (Fig. 4d-e), SEP was instead split at the median into upper (Q3-Q4) and lower (Q1-Q2) halves, so that the compared groups are mutually exclusive and jointly cover the full population, a condition for interpreting Gini and Theil as population-level distributional measures. Residence permit groups (settled: Swiss citizens and C-permit holders; temporary: B and L permit holders) are identical across both analyses.

Log-linear cooling gradient and saturation distance

Log-linear cooling gradient. To visualize how group-level cooling benefits vary with neighborhood extent, we fitted a log-linear model of the form $Coolingbenefit(r) = \alpha + \beta \cdot ln(r)$ to group-median cooling benefit at 50 focal radii (20-1,000 m in 20 m steps), where r is the focal radius in meters. The model was fitted by ordinary least squares. Fitted curves are shown in Fig. 2c.

Cooling saturation distance. The saturation distance (r_{95}) was derived from an exponential saturation model fitted independently to the group-median cooling profile. For each sociodemographic group, the model

$$\text{Cooling benefit}(r) = a \cdot (1 - \exp(-b \cdot r)) \tag{1}$$

was fitted by nonlinear least squares to the group-median cooling benefit at radii larger than 20 m (i.e., 40-1000 m in 20 m steps; up to 50,000 individuals per group), where a is the asymptotic maximum cooling and b is the rate parameter. The saturation distance was then derived analytically as:

$$r_{95} = \frac{-\ln(1 - 0.95)}{b} = \frac{\ln(20)}{b} \tag{2}$$

Group differences in r_{95} were assessed by a permutation test, and bootstrap standard errors were estimated as described above. r_{95} values are shown in Fig. 2b; standard errors are reported in Table S4. Full model parameter estimates per sociodemographic group are provided in Table S4.

Multiple regression analysis

To disentangle independent sociodemographic association with cooling, we estimated a pooled ordinary least squares (OLS) regression of individual-level tree-induced cooling at a focal radius of 100 m on all five sociodemographic indicators simultaneously. Categorical variables were dummy-coded with the following reference groups: age 65-79 years, Swiss citizens (permit type), high SEP, male (gender), and married (civil status). The model was estimated on n = 7,064,396 individuals with complete records across all indicators, after excluding missing, “Not specified”, and “Other” in residence permit categories. Regression coefficients, 95% confidence intervals, and significance (t-test) were reported for each non-reference level. Model fit was assessed with R^2 and the F-statistic. Results are presented as a forest plot (Fig. S5). The full regression table (β, SE, 95% CI, t, p, R^2, F-statistic) is provided in Table S5.

Group comparisons and bootstrap significance testing

To test for statistically significant differences in cooling benefit between sociodemographic groups, we used two complementary procedures depending on the outcome. For cooling magnitude at a specific focal radius (Fig. 2a), pairwise differences between each group and its reference were assessed by bootstrap resampling under the null hypothesis (2,000 resamples drawn with replacement; maximum 50,000 individuals per group): the focal and reference groups were pooled before each draw, and the two-sided p-value was taken as the proportion of null differences in group medians whose absolute value equalled or exceeded the observed absolute difference. For the saturation distance r_{95} (Fig. 2b), a permutation test was used: individuals from each group and its reference were pooled and randomly re-split into two groups of the original sizes; r_{95} was recomputed for each pseudo-split (500 permutations); the p-value was the proportion of absolute permutation differences that equaled or exceeded the observed absolute difference. Fewer iterations were used for r95 because each iteration requires re-fitting the exponential saturation model. For both procedures, p-values are reported as (r+1)/(B+1), which bounds the smallest resolvable value at 0.0005 for cooling magnitude (B = 2,000) and 0.002 for r95 (B = 500). Bootstrap standard errors for r_{95} were estimated separately from 200 within-group resamples (std of valid r_{95} estimates). All comparisons used the same reference groups for each indicator: age 65-79 years, Swiss citizens (permit type), high SEP, male (gender), and married (civil status).

Density-stratified analysis

To test whether sociodemographic disparities in cooling are confounded by residential density, we stratified individuals into three density tertiles (Low, Medium, and High) based on the focal population at the 100 m residential scale. Focal population was computed for each 100 m grid cell as the sum of residents in the cell and its four cardinal neighbors (north, south, east, west). Cells with fewer than five residents were excluded. Tertile boundaries were defined globally across all urban and peri-urban individuals. Within each stratum, group medians and interquartile ranges of cooling at 100 m were computed, and pairwise bootstrap significance tests (n = 2,000 resamples; maximum 50,000 individuals per group) were performed against the same reference groups used in the national analysis. Results are presented in Fig. S6. The same Group comparisons and bootstrap significance testing were applied within each density stratum in the density-stratified analysis (Fig. S6). Median cooling and bootstrap p-values per group × density stratum are provided in Table S6.

Scaling law analysis of cooling

We modelled the scaling of vegetation cooling benefits with population size using log-log ordinary least squares (OLS) regression:

$$Y = \alpha N^{\beta} \tag{3}$$

where *Y* is the mean individual cooling benefit (or inequality metric) at a given focal radius, N is the population count, α is a normalization constant, and β is the scaling exponent. The scaling exponent β represents the elasticity of the outcome with respect to population; a negative β indicates that cooling (or inequality) declines with increasing urban density or city size. Analyses were conducted at two spatial levels. At the 1 km^2 cell level, N is the cell population count, equivalent to population density (persons km^{-2}). At the municipality level, N is the total municipal population. Spatial units with fewer than 20 persons were excluded.

Group-specific scaling models were estimated for three stratifications: (1) Distributional: Y was the 10^{th} percentile (P10) and 90^{th} percentile (P90) of individual cooling within each spatial unit; (2) SEP: Y was the mean cooling of residents in the top (high SEP) or bottom (low SEP) national quartile of Swiss-SEP scores; (3) Residence permit: Y was the mean cooling of settled residents (Swiss citizens and C permit holders) or temporary residents (B and L permit holders). Group-specific models were restricted to spatial units containing at least 5 persons in each group. To formally test whether scaling exponents differ between social groups, we applied a within-unit ratio regression:

$$\ln\left(\frac{Y_1}{Y_2}\right) \sim \ln(N) \tag{4}$$

where the slope $\Delta\beta = \beta_1 - \beta_2$.

All models were estimated with heteroskedasticity-consistent HC3 robust standard errors (R packages *sandwich* and *lmtest*). Scaling analyses at both spatial levels (1 km² and municipality) were repeated at 10 focal radii from 100 to 1,000 m in 100 m intervals to assess robustness across spatial extents.

Inequality and equity typology analysis

Inequality metrics. Cooling inequality within each spatial unit was quantified using two complementary metrics. The Gini index measures overall dispersion in individual cooling exposure and was computed using the sorted-ranks formula:

$$Gini = 1 + \frac{1}{n} - \left(\frac{2}{(n^2\mu)}\right)\sum_i (n + 1 - i)\, x_{(i)} \tag{5}$$

where $x_{(i)}$ is individual cooling exposures sorted in ascending order, μ is the mean cooling exposure, and *n* is the population size. The Theil index, an entropy-based alternative to the Gini, was computed

as:

$$Theil = \frac{1}{n\sum_i\left(\frac{x_i}{\mu}\right) ln\left(\frac{x_i}{\mu}\right)} \tag{6}$$

where x_i is the cooling exposure of individual *i* and μ is the population mean. Both metrics were computed at the individual level within each spatial unit (1 km² cell and municipality) across all focal radii.

Concentration Index. The Concentration Index (CI) assesses whether cooling is systematically distributed in favor of socially advantaged or disadvantaged residents. We used the two-group rank-based formulation:

$$CI = \frac{\left(2(w_1 r_1 \mu_1 + w_2 r_2 \mu_2)\right)}{\mu} - 1 \tag{7}$$

where the population is divided into two groups, a socially advantaged group (group 1) and a socially disadvantaged group (group 2), defined separately for each indicator: upper 50% versus lower 50% SEP, permanent versus temporary residents, and the 65-79 versus 80+ age groups. Here w_1 and w_2 are the population shares of each group ($w_1 + w_2 = 1$), μ_1 and μ_2 are their mean cooling exposures, and μ is the overall mean cooling. The fractional ranks are assigned as $r_2 = w_2/2$ (disadvantaged group, ranked below) and $r_1 = w_2 + w_1/2$ (advantaged group, ranked above), placing the disadvantaged group at the lower end of the social rank distribution. A positive CI indicates that cooling is disproportionately concentrated among the advantaged group (pro-advantaged); a negative CI indicates higher cooling benefits among the disadvantaged group (pro-disadvantaged). A minimum of 5 individuals per group was required for CI computation.

Municipal-level equity diagnostics. Each municipality was characterized by its Gini index (overall cooling dispersion) and CI (social bias in cooling). Municipalities were classified into four quadrants by whether their Gini exceeded the cross-municipality mean and whether their CI was positive (pro-advantaged) or negative (pro-disadvantaged). High Gini combined with positive CI (upper-right quadrant) indicates that cooling is both unevenly distributed and concentrated among advantaged residents (least equitable); low Gini combined with negative CI (lower-left quadrant) reflects more equitable, pro-disadvantaged conditions. The same classification was applied at the 1 km^2 cell level to produce a national equity typology map.

Data availability

The vegetation and land-surface datasets used for modeling tree-induced cooling include the 1 m Vegetation Height Model from the National Forest Inventory (NFI, last accessed 30 October 2024; the old website is closed, and currently the dataset is available at https://www.envidat.ch/dataset/vegetation-height-model-nfi). The Leaf Area Index (LAI, 300 m) is from the Copernicus Global Land Service (https://land.copernicus.eu/en/products/vegetation/leaf-area-index-300m-v1.0). Habitat and land-cover data were derived from the Habitat Map of Switzerland (https://www.envidat.ch/#/metadata/habitat-map-of-switzerland). Meteorological variables used in the rSCOPE model were sourced from the ERA5 reanalysis produced by the

Copernicus Climate Data Store (CDS; https://cds.climate.copernicus.eu/). Hourly variables included 2 m temperature, 10 m wind speed, surface pressure, total precipitation, downward shortwave and longwave radiation, and relative humidity. ERA5 data were accessed via the *ecmwfr* interface in R. All ERA5 data were retrieved for the full year 2018, cropped to the Swiss domain, and reprojected to match the model coordinate reference system. The outcome datasets of cooling benefits from urban vegetation generated in this study are deposited in the ETH Zurich Research Collection (https://www.research-collection.ethz.ch/entities/researchdata/022ab0f4-18ef-4c3a-a7d3-3e206daaafbd, under embargo). The biogeographical regions of Switzerland were obtained from the Swiss Geographic Catalogue (https://www.geocat.ch/geonetwork/srv/eng/catalog.search#/metadata/fc110d43-cfbc-4029-a73c-f24bd67c9689). Individual- and micro-neighborhood- level demographic data were obtained from Swiss Federal Statistical Office (https://www.bfs.admin.ch/bfs/en/home/statistiken/bevoelkerung/erhebungen/statpop.html). All demographic datasets above were accessed under a data-sharing agreement with the Swiss Federal Statistical Office, in compliance with the Swiss Federal Act on Data Protection (FADP) and applicable data confidentiality regulations. The record linkage was performed by the FSO, and the matched dataset was made available to the researchers in an anonymized/pseudonymized format and cannot be shared.

Code availability

Vegetation cooling was simulated with the SCOPE model as implemented in the rSCOPE R package (v1.0)[66]. All subsequent processing and analysis were performed in Python and R. Processing of the 1 m national canopy height data, individual-level cooling extraction, and the bootstrap and permutation procedures were run on the ETH Zurich Euler high-performance computing cluster. Although the underlying individual-level records cannot be shared under the data agreement with the Swiss Federal Statistical Office, the analysis code will be deposited in a public repository (Zenodo) and made openly available upon publication.

Acknowledgements

This work was supported by ETH Zurich. We gratefully acknowledge the Swiss Federal Statistical Office for its assistance in arranging the data agreement and transferring the STATPOP and Swiss National Cohort datasets. We also acknowledge the ETH High-Performance Computing Cluster (Euler) for providing the computational infrastructure. We acknowledge the support from the National Council for Scientific and Technological Development – CNPq under the programme Conhecimento Brasil Grant [446437/2024-7] to A.D.R.

Author Contributions

Y.C. and F.K. conceived and designed the study, with G.M., J.S., and J.G. contributing to conceptualization. Y.C. performed data collection and analysis, with contributions from A.D.R. to model development. Y.C. drafted the manuscript. J.G. acquired funding. F.K., G.M., J.S., A.D.R., M.J.S., D.A.M., R.B., and J.G. contributed to manuscript review and editing.

Declaration of Generative AI and AI-assisted technologies in the writing process

During the writing process of this work, we used OpenAI's ChatGPT to improve the language for clarity and conciseness. After using this tool, we thoroughly reviewed and edited the manuscript, and we take full responsibility for the content of the publication.

References

1. Richards, D. R. *et al.* Global variation in contributions to human well-being from urban vegetation ecosystem services. *One Earth* **5**, 522–533 (2022).
2. Wong, N. H., Tan, C. L., Kolokotsa, D. D. & Takebayashi, H. Greenery as a mitigation and adaptation strategy to urban heat. *Nat Rev Earth Environ* **2**, 166–181 (2021).
3. Anguelovski, I., Kotsila, P., Lees, L., Triguero-Mas, M. & Calderón-Argelich, A. From heat racism and heat gentrification to urban heat justice in the USA and Europe. *Nat Cities* **2**, 8–16 (2025).
4. Hsu, A., Sheriff, G., Chakraborty, T. & Manya, D. Disproportionate exposure to urban heat island intensity across major US cities. *Nat Commun* **12**, 2721 (2021).
5. Kleinschroth, F. *et al.* Global disparities in urban green space use during the COVID-19 pandemic from a systematic review. *Nat Cities* 1–14 (2024) doi:10.1038/s44284-023-00020-6.
6. Li, Y. *et al.* Green spaces provide substantial but unequal urban cooling globally. *Nat Commun* **15**, 7108 (2024).
7. Wolch, J. R., Byrne, J. & Newell, J. P. Urban green space, public health, and environmental justice: The challenge of making cities 'just green enough'. *Landscape and Urban Planning* **125**, 234–244 (2014).
8. Tuholske, C. *et al.* Global urban population exposure to extreme heat. *Proceedings of the National Academy of Sciences* **118**, e2024792118 (2021).
9. Iungman, T. *et al.* Cooling cities through urban green infrastructure: a health impact assessment of European cities. *The Lancet* **401**, 577–589 (2023).
10. Zhao, J., Zhao, X., Wu, D., Meili, N. & Fatichi, S. Satellite-based evidence highlights a considerable increase of urban tree cooling benefits from 2000 to 2015. *Global Change Biology* **29**, 3085–3097 (2023).
11. Zhang, Y. *et al.* Transfer learning reveals large discrepancies between air and land surface temperatures in cities. *Nat Commun* https://doi.org/10.1038/s41467-026-73716-7 (2026) doi:10.1038/s41467-026-73716-7.
12. Wu, Z. & Chen, L. Optimizing the spatial arrangement of trees in residential neighborhoods for better cooling effects: Integrating modeling with in-situ measurements. *Landscape and Urban Planning* **167**, 463–472 (2017).
13. Yang, Y. *et al.* Regulation of humid heat by urban green space across a climate wetness gradient. *Nat Cities* **1**, 871–879 (2024).

14. Tsoka, S., Tsikaloudaki, A. & Theodosiou, T. Analyzing the ENVI-met microclimate model's performance and assessing cool materials and urban vegetation applications–A review. *Sustainable Cities and Society* **43**, 55–76 (2018).
15. Huang, W. T. K. *et al.* Economic valuation of temperature-related mortality attributed to urban heat islands in European cities. *Nat Commun* **14**, 7438 (2023).
16. Sayyed, T. K. *et al.* Satellite data for environmental justice: a scoping review of the literature in the United States. *Environ. Res. Lett.* **19**, 033001 (2024).
17. Buzzelli, M. Modifiable Areal Unit Problem. in *International Encyclopedia of Human Geography (Second Edition)* (ed. Kobayashi, A.) 169–173 (Elsevier, Oxford, 2020). doi:10.1016/B978-0-08-102295-5.10406-8.
18. Ziter, C. D., Pedersen, E. J., Kucharik, C. J. & Turner, M. G. Scale-dependent interactions between tree canopy cover and impervious surfaces reduce daytime urban heat during summer. *Proceedings of the National Academy of Sciences* **116**, 7575–7580 (2019).
19. Wüstemann, H., Kalisch, D. & Kolbe, J. Access to urban green space and environmental inequalities in Germany. *Landscape and Urban Planning* **164**, 124–131 (2017).
20. Bettencourt, L. M. A. The Origins of Scaling in Cities. *Science* **340**, 1438–1441 (2013).
21. Bettencourt, L. & West, G. A unified theory of urban living. *Nature* **467**, 912–913 (2010).
22. Bettencourt, L. M. A., Lobo, J., Helbing, D., Kühnert, C. & West, G. B. Growth, innovation, scaling, and the pace of life in cities. *Proceedings of the National Academy of Sciences* **104**, 7301–7306 (2007).
23. Succar, R. & Porfiri, M. Urban scaling of firearm violence, ownership and accessibility in the United States. *Nat Cities* **1**, 216–224 (2024).
24. Xu, Y., Olmos, L. E., Abbar, S. & González, M. C. Deconstructing laws of accessibility and facility distribution in cities. *Science Advances* **6**, eabb4112 (2020).
25. Lu, M., Zhou, C., Wang, C., Jackson, R. B. & Kempes, C. P. Worldwide scaling of waste generation in urban systems. *Nat Cities* **1**, 126–135 (2024).
26. Lamsal, L. N., Martin, R. V., Parrish, D. D. & Krotkov, N. A. Scaling Relationship for NO2 Pollution and Urban Population Size: A Satellite Perspective. *Environ. Sci. Technol.* **47**, 7855–7861 (2013).
27. Arvidsson, M., Lovsjö, N. & Keuschnigg, M. Urban scaling laws arise from within-city inequalities. *Nat Hum Behav* **7**, 365–374 (2023).

28. Pandey, B., Brelsford, C. & Seto, K. C. Infrastructure inequality is a characteristic of urbanization. *Proceedings of the National Academy of Sciences* **119**, e2119890119 (2022).
29. Duran-Sala, M., Hendrick, M. & Manoli, G. Scaling intra-urban climate fluctuations. *Nat Cities* **3**, 545–554 (2026).
30. Ballester, J. *et al.* Heat-related mortality in Europe during the summer of 2022. *Nat Med* **29**, 1857–1866 (2023).
31. Rousi, E., Kornhuber, K., Beobide-Arsuaga, G., Luo, F. & Coumou, D. Accelerated western European heatwave trends linked to more-persistent double jets over Eurasia. *Nat Commun* **13**, 3851 (2022).
32. Ceppi, P., Scherrer, S. C., Fischer, A. M. & Appenzeller, C. Revisiting Swiss temperature trends 1959–2008. *International Journal of Climatology* **32**, 203–213 (2012).
33. Federal Statistical Office. *Current Situation and Change: Key Population Figures, 2025 (Provisional Annual Figures)*. https://www.bfs.admin.ch/bfs/en/home/statistics/population/effectif-change.html (2026).
34. Chang, Y., Manoli, G., Ghazoul, J. & Kleinschroth, F. Socio-demographic disparities of heat exposure in affluent, aging, and diverse Swiss society. *Sustainable Cities and Society* **132**, 106813 (2025).
35. Lanza, K. *et al.* Heat vulnerability of Latino and Black residents in a low-income community and their recommended adaptation strategies: A qualitative study. *Urban Climate* **51**, 101656 (2023).
36. Randazzo, T., De Cian, E. & Mistry, M. N. Air conditioning and electricity expenditure: The role of climate in temperate countries. *Economic Modelling* **90**, 273–287 (2020).
37. Chi, D. *et al.* Residential tree canopy configuration and mortality in 6 million Swiss adults: a longitudinal study. *The Lancet Planetary Health* **9**, e186–e195 (2025).
38. Duarte Rocha, A., Vulova, S., van der Tol, C., Förster, M. & Kleinschmit, B. Modelling hourly evapotranspiration in urban environments with SCOPE using open remote sensing and meteorological data. *Hydrology and Earth System Sciences* **26**, 1111–1129 (2022).
39. Stuhlmacher, M., Frazier, A. E., Corya, I. & Yang, W. As cities grow larger, they may also become less green. *Journal of Land Use Science* **20**, 176–196 (2025).
40. Molinero, C. & Thurner, S. How the geometry of cities determines urban scaling laws. *J R Soc Interface* **18**, 20200705 (2021).
41. Shang, L. *et al.* Scaling of multiple functional facilities covering comprehensive processes in cities. *Cities* **145**, 104666 (2024).

42. Chang, Y., van Strien, M. J., Zohner, C. M., Ghazoul, J. & Kleinschroth, F. Effects of climate, socioeconomic development, and greening governance on enhanced greenness under urban densification. *Resources, Conservation and Recycling* **206**, 107624 (2024).
43. McDonald, R. I. *et al.* Denser and greener cities: Green interventions to achieve both urban density and nature. *People and Nature* **5**, 84–102 (2023).
44. Esperon-Rodriguez, M. *et al.* Barriers and opportunities for resilient and sustainable urban forests. *Nat Cities* **2**, 290–298 (2025).
45. Gobatti, L., Bach, P. M., Maurer, M. & Leitão, J. P. Impact of soil moisture content on urban tree evaporative cooling and human thermal comfort. *npj Urban Sustain* **5**, 26 (2025).
46. Grêt-Regamey, A., Galleguillos-Torres, M., Dissegna, A. & Weibel, B. How urban densification influences ecosystem services—a comparison between a temperate and a tropical city. *Environ. Res. Lett.* **15**, 075001 (2020).
47. Seto, K. C., Sánchez-Rodríguez, R. & Fragkias, M. The New Geography of Contemporary Urbanization and the Environment. *Annual Review of Environment and Resources* **35**, 167–194 (2010).
48. Meili, N. *et al.* Tree effects on urban microclimate: Diurnal, seasonal, and climatic temperature differences explained by separating radiation, evapotranspiration, and roughness effects. *Urban Forestry & Urban Greening* **58**, 126970 (2021).
49. Rocha, A. D. *et al.* Unprivileged groups are less served by green cooling services in major European urban areas. *Nat Cities* **1**, 424–435 (2024).
50. Haandrikman, K., Costa, R., Malmberg, B., Rogne, A. F. & Sleutjes, B. Socio-economic segregation in European cities. A comparative study of Brussels, Copenhagen, Amsterdam, Oslo and Stockholm. *Urban Geography* **44**, 1–36 (2023).
51. Benz, S. A. & Burney, J. A. Widespread Race and Class Disparities in Surface Urban Heat Extremes Across the United States. *Earth's Future* **9**, e2021EF002016 (2021).
52. Chakraborty, T. C., Newman, A. J., Qian, Y., Hsu, A. & Sheriff, G. Residential segregation and outdoor urban moist heat stress disparities in the United States. *One Earth* **6**, 738–750 (2023).
53. Whitehead, M. The Concepts and Principles of Equity and Health. *Int J Health Serv* **22**, 429–445 (1992).
54. Masselot, P. *et al.* Estimating future heat-related and cold-related mortality under climate change, demographic and adaptation scenarios in 854 European cities. *Nat Med* **31**, 1294–1302 (2025).

55. Pavanello, F. *et al.* Air-conditioning and the adaptation cooling deficit in emerging economies. *Nat Commun* **12**, 6460 (2021).
56. Yin, Y., He, L., Wennberg, P. & Frankenberg, C. Unequal exposure to heatwaves in Los Angeles: Impact of uneven green spaces. *Science advances* **9**, eade8501 (2023).
57. Rocha, A. D., Vulova, S., Meier, F., Förster, M. & Kleinschmit, B. Mapping evapotranspirative and radiative cooling services in an urban environment. *Sustainable Cities and Society* **85**, 104051 (2022).
58. Hersbach, H. *et al.* The ERA5 global reanalysis. *Quarterly Journal of the Royal Meteorological Society* **146**, 1999–2049 (2020).
59. Flückiger, B. *et al.* Modelling daily air temperature at a fine spatial resolution dealing with challenging meteorological phenomena and topography in Switzerland. *Intl Journal of Climatology* **42**, 6413–6428 (2022).
60. Fuster, B. *et al.* Quality Assessment of PROBA-V LAI, fAPAR and fCOVER Collection 300 m Products of Copernicus Global Land Service. *Remote Sensing* **12**, 1017 (2020).
61. Price, B., Huber, N., Nussbaumer, A. & Ginzler, C. The Habitat Map of Switzerland: A Remote Sensing, Composite Approach for a High Spatial and Thematic Resolution Product. *Remote Sensing* **15**, 643 (2023).
62. Vienneau, D. *et al.* Transportation noise exposure and cardiovascular mortality: 15-years of follow-up in a nationwide prospective cohort in Switzerland. *Environment International* **158**, 106974 (2022).
63. Panczak, R., Berlin, C., Voorpostel, M., Zwahlen, M. & Egger, M. The Swiss neighbourhood index of socioeconomic position: update and re-validation. *Swiss Medical Weekly* **153**, 40028–40028 (2023).
64. Federal Statistical Office. Typology of municipalities and urban-rural typology. (2017).
65. van der Tol, C., Verhoef, W., Timmermans, J., Verhoef, A. & Su, Z. An integrated model of soil-canopy spectral radiances, photosynthesis, fluorescence, temperature and energy balance. *Biogeosciences* **6**, 3109–3129 (2009).
66. Rocha, A. D. AlbyDR/rSCOPE: rSCOPE v1.0. https://doi.org/10.5281/zenodo.6204580 (2022) doi:10.5281/zenodo.6204580.

Supplementary information

"Unequal scaling of urban vegetation cooling across sociodemographic groups"

Contents

Figures

Tables

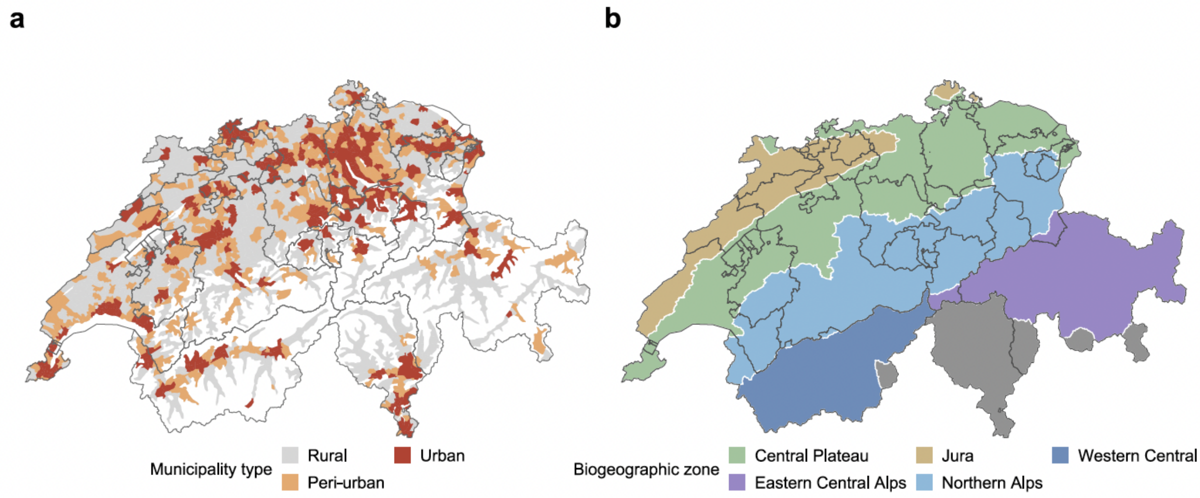

Fig. S1. Study area overview. (a) Classification of Swiss municipalities into Rural (grey), Peri-urban (orange), and Urban (red) categories based on the Swiss Federal Statistical Office urbanization typology. Study municipalities are overlaid on the full Swiss municipal boundary layer; cantonal borders are shown in dark grey. (b) Biogeographic zones of Switzerland, comprising six regions: Central Plateau, Jura, Northern Alps, Western Central Alps, Eastern Central Alps, and Southern Alps.

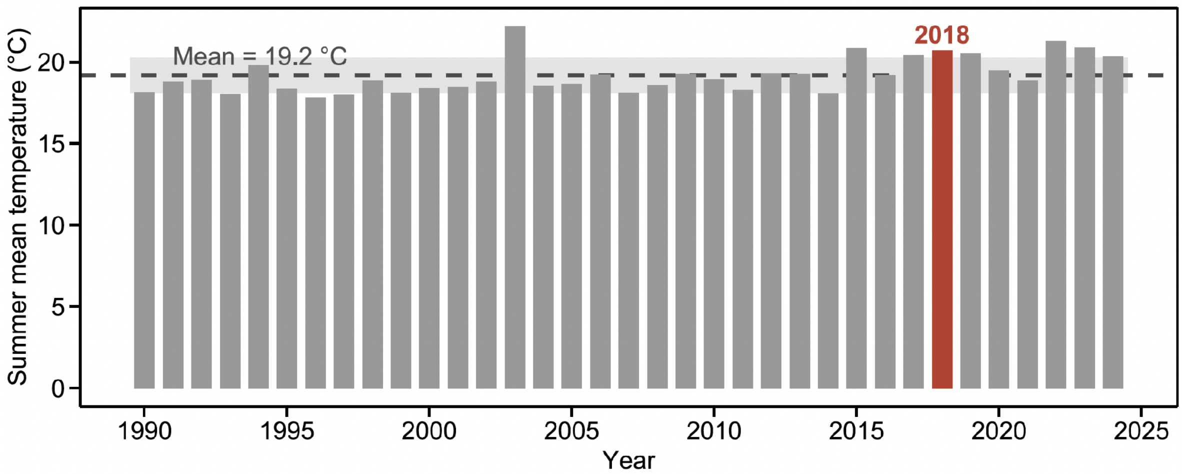

Fig. S2. Historical summer (June-August) mean temperature across Switzerland from 1990 to 2024. Averaged across nine MeteoSwiss National Basic Climatological Network (NBCN) homogenized station records (Basel/Binningen, Bern/Zollikofen, Geneva/Cointrin, Lugano, Lucerne, Zürich/Fluntern, Sion, Neuchâtel, and St. Gallen). The dashed line indicates the 1990-2024 long-term mean (19.2 °C); the shaded band denotes ±1 standard deviation. The study year 2018 (red bar) slightly exceeds the upper bound of the ±1 standard deviation range, indicating a warm but not extreme summer relative to the recent climatological baseline.

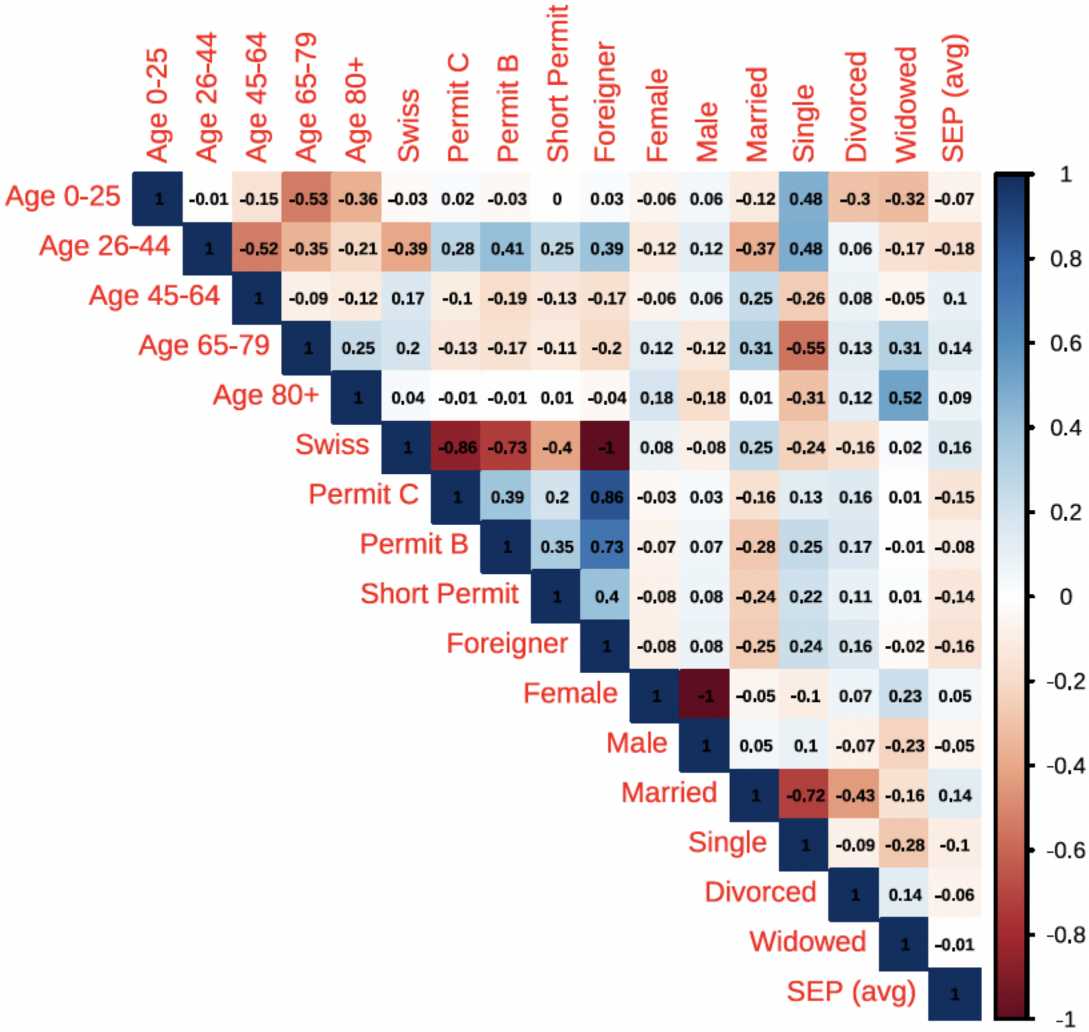

Fig. S3. Pairwise Spearman rank correlation matrix among the five sociodemographic indicators used in the main analysis (age, gender, civil status, residence permit type, and socioeconomic position). Nationality and residence permit type show the highest inter-indicator correlation, motivating the exclusion of nationality from the main analysis.

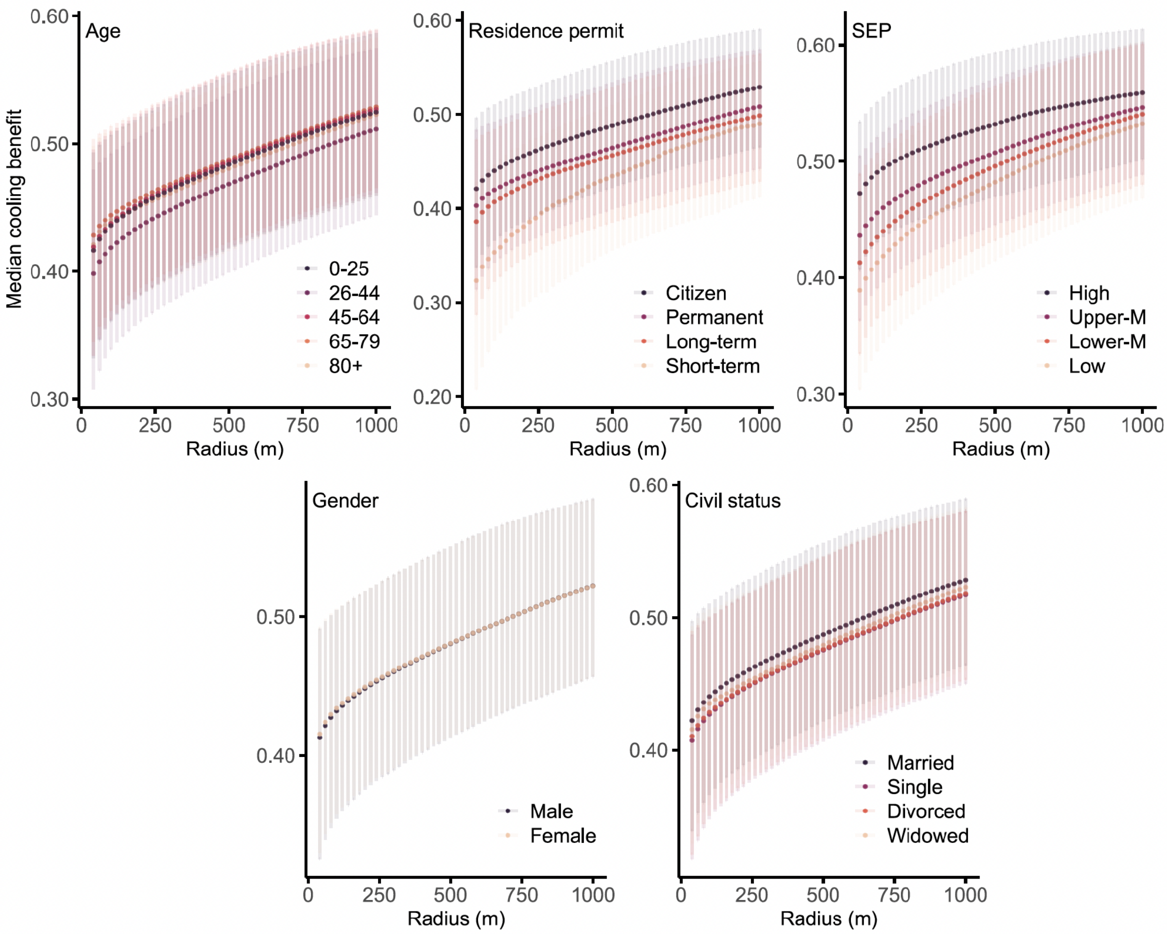

Fig. S4. Observed medians and interquartile ranges at each focal radius, before fitting. Dots represent medians, shades represent the distribution from 25th (lower) to 75th (upper).

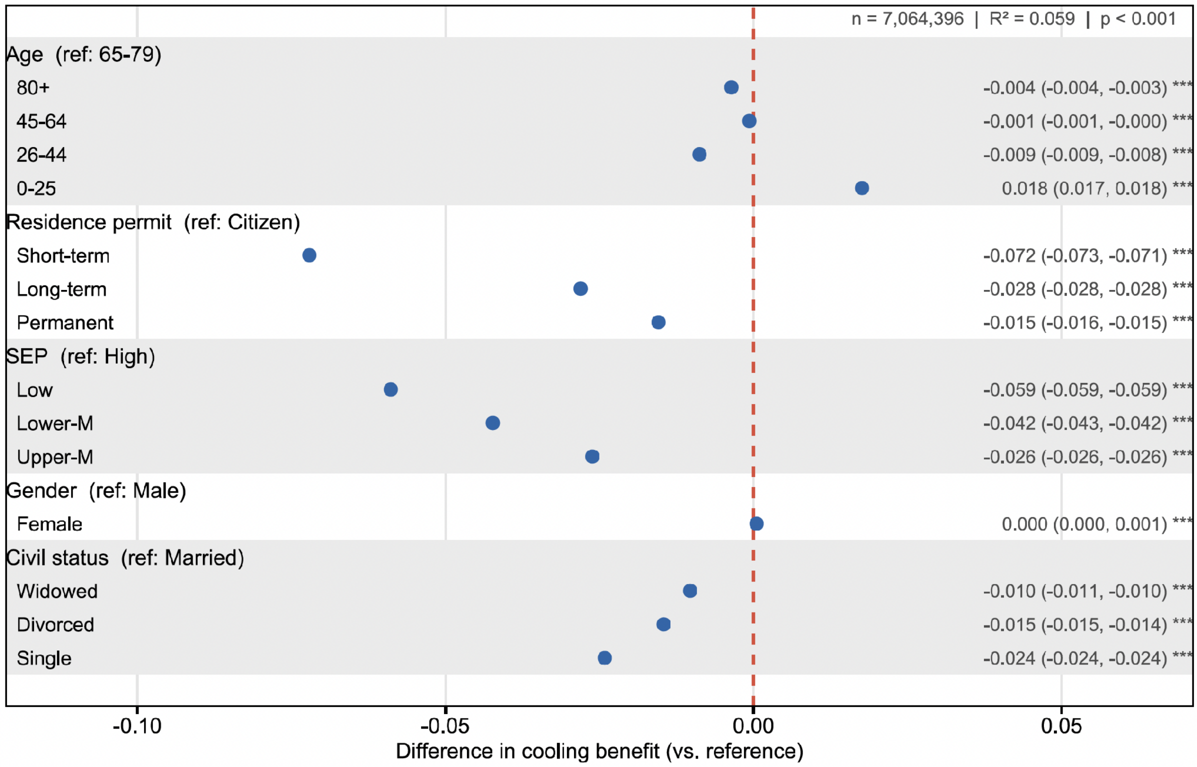

Fig. S5. Multiple regression of individual-level cooling benefit (cooling benefits at 100 m focal radius) on five simultaneously included sociodemographic predictors. Forest plot of regression coefficients (β) with 95% confidence intervals for each non-reference group. Reference groups are shown in parentheses. Significance: *** $p < 0.001$, ** $p < 0.01$, * $p < 0.05$, ns not significant.

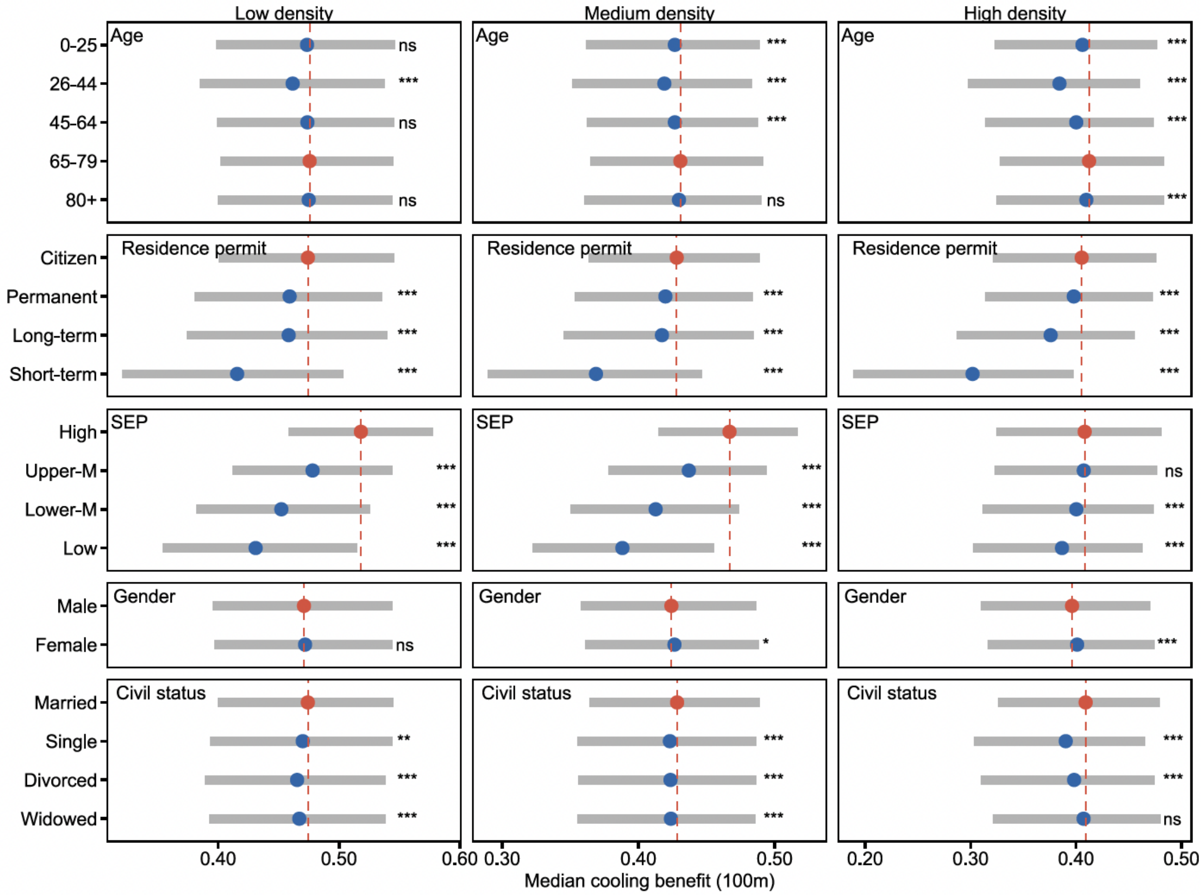

Fig. S6. Density-stratified sociodemographic disparities in cooling benefit at a focal radius of 100 m. Groups are compared within three population density strata (Low, Medium, High) defined by tertiles of focal population at the 100 m scale. Points indicate group medians; horizontal bars denote interquartile ranges. Significance stars show bootstrap pairwise tests versus the reference group within each stratum (*** $p < 0.001$, ** $p < 0.01$, * $p < 0.05$, ns not significant). The consistency of group rank orderings across strata confirms that the observed disparities are not artefacts of density confounding.

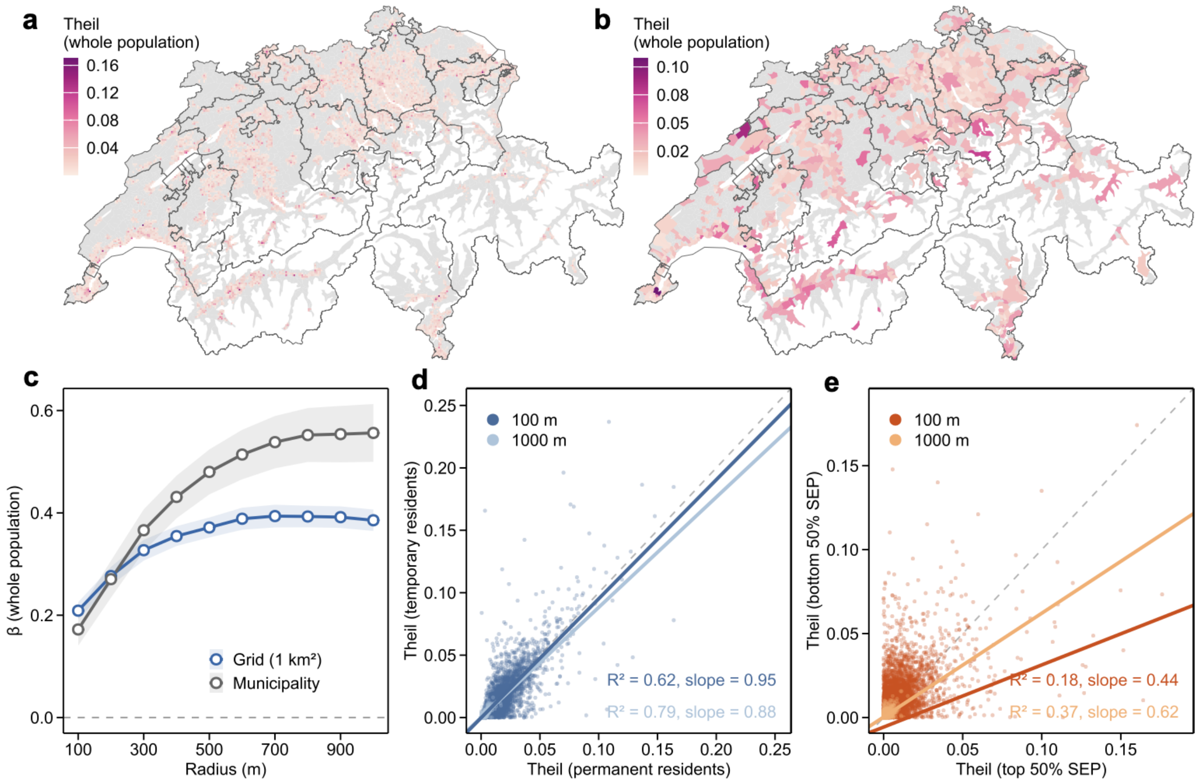

Fig. S7. Urban scaling of cooling inequality measured by the Theil index. a-b, Spatial distribution of the Theil index at the 1km^2 level (a) and municipality level (b), computed at a 100 m focal radius. c, Scaling exponent (β) of the Theil index against population size, estimated separately at the 1 km² cell (filled circles) and municipality (open circles) levels across focal radii from 100 to 1,000 m (100 m steps); the dashed horizontal line indicates β = 0; shaded ribbons show 95% confidence intervals. d-e, Pairwise comparison of subgroup Theil values at the 1 km² cell level, shown at focal radii of 100 m (dark) and 1,000 m (light), for permit type groups (d) and SEP groups (e); solid lines show ordinary least squares regression fits with reported slope and R² values.

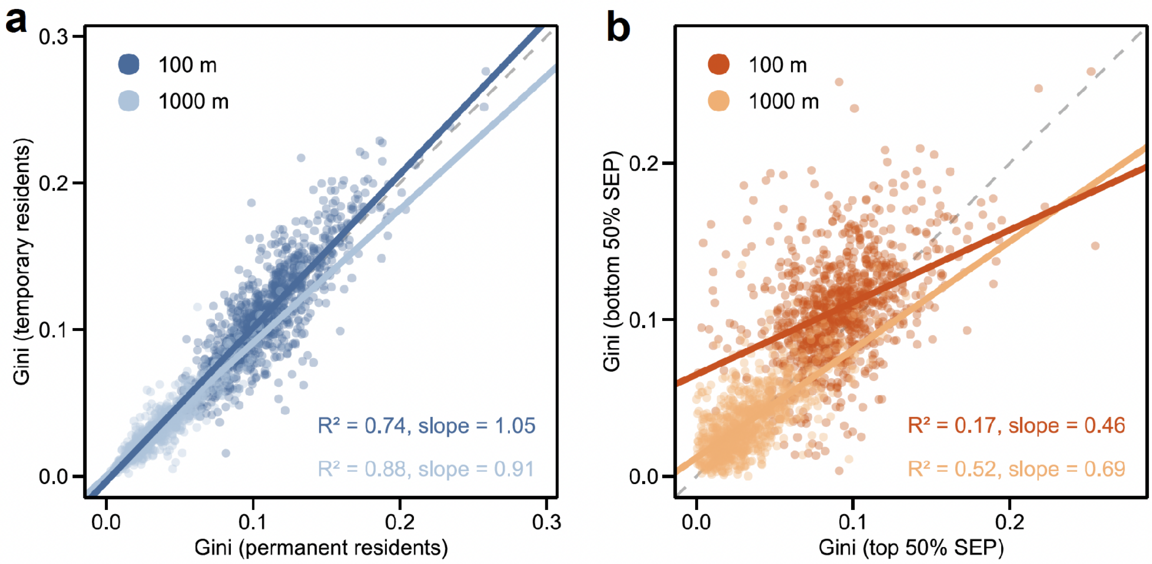

Fig. S8. Pairwise comparison of cooling inequality (Gini index) between social groups at focal radii of 100 m and 1000 m at municipality level. a, Gini index for temporary residents versus permanent residents. b, Gini index for residents in the bottom 50% versus the top 50% of socioeconomic position (SEP). Dashed lines indicate the 1:1 equality line; solid lines show ordinary least squares regression fits with reported slope and R^2 values. Points above the 1:1 line indicate higher cooling inequality for the group on the y-axis.

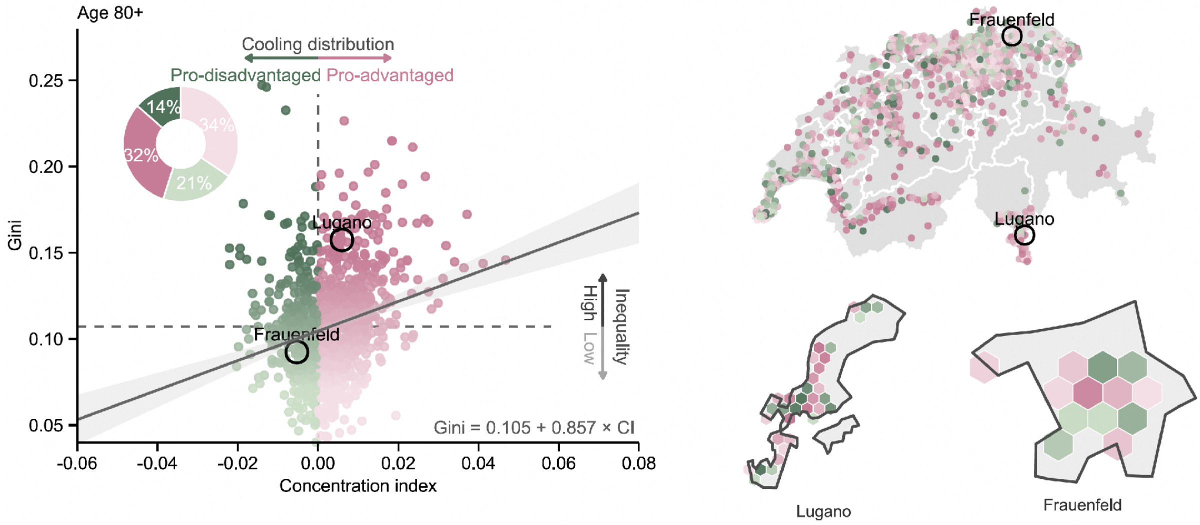

Fig. S9. Municipal-level characterization of cooling inequality and equity for the elderly population (aged 65-79 versus 80+) across Swiss urban and peri-urban municipalities. Left panel: each point represents one municipality in Gini-CI space; the Gini index (y-axis) is derived from individual-level 100 m focal cooling and the Concentration Index (CI; x-axis) is computed from 1 km² cells weighted by the population share of residents aged 80 and above. Negative CI values indicate cooling concentrated among the 65-79; positive CI values indicate pro-elderly (aged 80+) cooling. Dashed lines mark the mean Gini (horizontal) and CI = 0 (vertical); insets show the percentage of municipalities in each quadrant. In the figure, "high" and "low" inequality refer to Gini values above and below this cross-municipality mean, corresponding to above- and below-average inequality in the main text. The regression line shows the fitted linear relationship with 95% confidence interval. Right panel: geographic distribution of municipalities colored by Gini-CI quadrant classification; red = upper-left quadrant (above-average inequality, pro-privileged); green = lower-right quadrant (below-average inequality, pro-vulnerable). Canton boundaries are shown in white. Annotated examples illustrate contrasting municipal profiles: Lugano (Ticino) in the pro-privileged, above-average inequality quadrant; Frauenfeld (Thurgau) in the pro-vulnerable, below-average inequality quadrant.

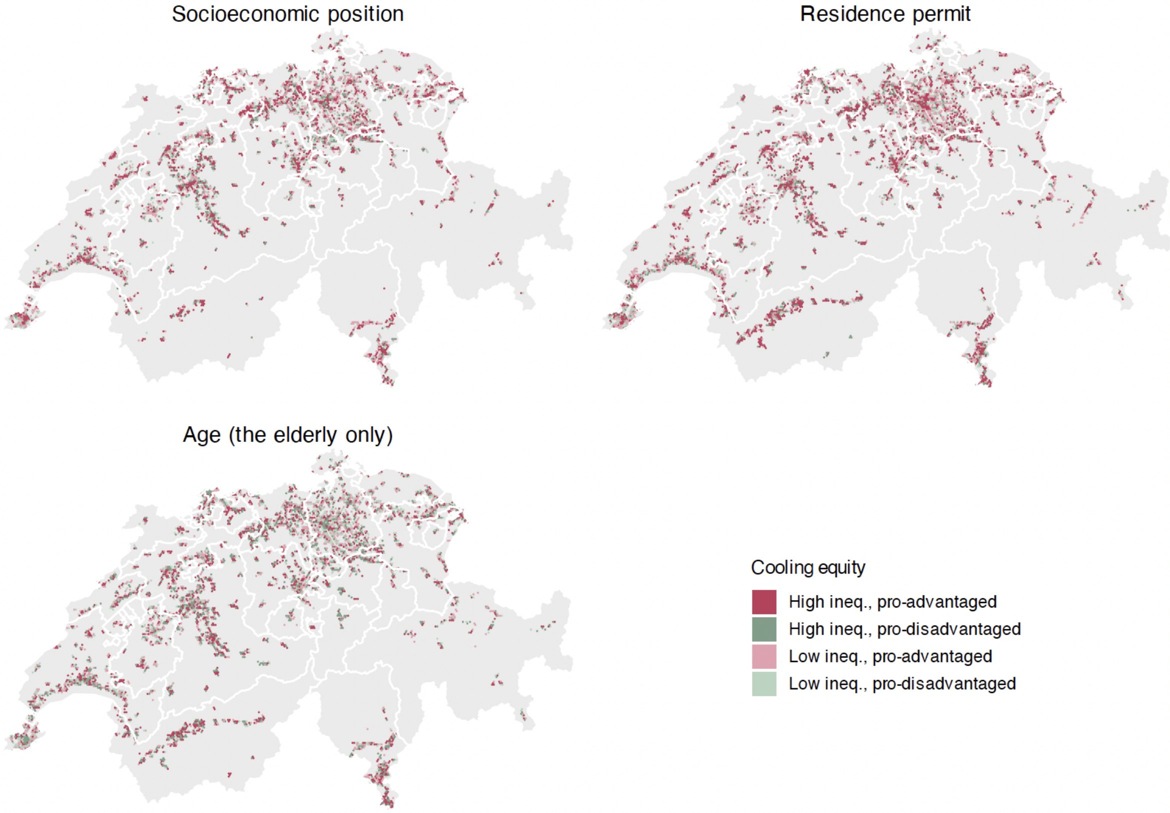

Fig. S10. National distribution of cooling equity typology at the cell scale (1 km²). Each cell is classified into one of four quadrants defined by its Gini index (internal inequality in cooling exposure; horizontal threshold = national mean) and Concentration Index (CI; vertical threshold = 0). Positive CI indicates cooling is concentrated among socioeconomically advantaged residents (pro-advantaged); negative CI indicates the reverse. in the figure, "high" and "low" inequality refer to Gini values above and below this cross-municipality mean, corresponding to above- and below-average inequality in the main text. Panels show classifications based on (a) socioeconomic position (SEP), (b) residence permit status, and (c) age group (residents aged 80+ versus 65-79). Only cells with ≥ 20 residents and valid Gini estimates are shown. Canton boundaries shown in white.

Table S1. Pairwise bootstrap significance tests for group differences in cooling benefit at a focal radius of 100 m. For each sociodemographic indicator, each non-reference group is compared to the reference group (*italicized*) by pooling the two groups and resampling under the null hypothesis (2,000 resamples; max 50,000 individuals per group). The p-value is the proportion of null differences whose absolute value equals or exceeds the observed absolute difference.

Indicator	Group	n	Observed Δ GCoS	p-value
Age group	*65–79 (ref.)*	—	—	—
Age group	0–25	50,000	-0.009	<0.001
Age group	26–44	50,000	-0.026	<0.001
Age group	45–64	50,000	-0.006	<0.001
Age group	≥80	50,000	-0.004	<0.001
Residence permit	*Swiss citizen (ref.)*	—	—	—
Residence permit	Long-term (B)	50,000	-0.032	<0.001
Residence permit	Permanent (C)	50,000	-0.020	<0.001
Residence permit	Short-term (L)	50,000	-0.086	<0.001
Gender	*Male (ref.)*	—	—	—
Gender	Female	50,000	0.001	0.439
Civil status	*Married (ref.)*	—	—	—
Civil status	Divorced	50,000	-0.011	<0.001
Civil status	Single	50,000	-0.012	<0.001
Civil status	Widowed	50,000	-0.005	<0.001
Socioeconomic position	*High (ref.)*	—	—	—
Socioeconomic position	Low	50,000	-0.072	<0.001
Socioeconomic position	Lower-middle	50,000	-0.050	<0.001
Socioeconomic position	Upper-middle	50,000	-0.031	<0.001

Table S2. Urban scaling exponents (β) for cooling inequality (Gini and Theil indices) at cell level (1 km²) and municipality level across focal radii (100–1000 m). β estimated by OLS regression of log(index) on log(population) with HC3 robust standard errors. 95% CI = heteroscedasticity-robust confidence interval; R^2 = coefficient of determination; p = two-sided p-value; n = number of spatial units.

Radius (m)	Scale	Index	β	95% CI	R^2	p	n
100	Cell (1 km²)	Gini	0.126	[0.112, 0.141]	0.052	<0.001	8055
200	Cell (1 km²)	Gini	0.153	[0.142, 0.164]	0.126	<0.001	8053
300	Cell (1 km²)	Gini	0.177	[0.167, 0.187]	0.142	<0.001	8055
400	Cell (1 km²)	Gini	0.201	[0.186, 0.217]	0.118	<0.001	8058
500	Cell (1 km²)	Gini	0.210	[0.196, 0.224]	0.124	<0.001	8059
600	Cell (1 km²)	Gini	0.210	[0.198, 0.222]	0.165	<0.001	8057
700	Cell (1 km²)	Gini	0.216	[0.203, 0.230]	0.143	<0.001	8058
800	Cell (1 km²)	Gini	0.224	[0.209, 0.240]	0.115	<0.001	8060
900	Cell (1 km²)	Gini	0.218	[0.204, 0.232]	0.137	<0.001	8058
1000	Cell (1 km²)	Gini	0.215	[0.201, 0.228]	0.135	<0.001	8058
100	Municipality	Gini	0.083	[0.068, 0.099]	0.104	<0.001	1021
200	Municipality	Gini	0.139	[0.121, 0.158]	0.196	<0.001	1021
300	Municipality	Gini	0.192	[0.171, 0.213]	0.263	<0.001	1021
400	Municipality	Gini	0.229	[0.207, 0.251]	0.302	<0.001	1021
500	Municipality	Gini	0.256	[0.233, 0.278]	0.314	<0.001	1021
600	Municipality	Gini	0.274	[0.249, 0.299]	0.316	<0.001	1021
700	Municipality	Gini	0.287	[0.261, 0.313]	0.307	<0.001	1021
800	Municipality	Gini	0.293	[0.266, 0.320]	0.295	<0.001	1021
900	Municipality	Gini	0.293	[0.266, 0.321]	0.279	<0.001	1021
1000	Municipality	Gini	0.293	[0.264, 0.321]	0.267	<0.001	1021
100	Cell (1 km²)	Theil	0.209	[0.192, 0.225]	0.094	<0.001	8053
200	Cell (1 km²)	Theil	0.277	[0.259, 0.294]	0.120	<0.001	8055
300	Cell (1 km²)	Theil	0.327	[0.307, 0.347]	0.141	<0.001	8057
400	Cell (1 km²)	Theil	0.355	[0.335, 0.374]	0.154	<0.001	8057
500	Cell (1 km²)	Theil	0.371	[0.352, 0.391]	0.167	<0.001	8057
600	Cell (1 km²)	Theil	0.389	[0.367, 0.410]	0.153	<0.001	8060
700	Cell (1 km²)	Theil	0.394	[0.372, 0.416]	0.156	<0.001	8059
800	Cell (1 km²)	Theil	0.393	[0.372, 0.414]	0.159	<0.001	8057
900	Cell (1 km²)	Theil	0.392	[0.371, 0.413]	0.150	<0.001	8058
1000	Cell (1 km²)	Theil	0.386	[0.365, 0.406]	0.146	<0.001	8058
100	Municipality	Theil	0.172	[0.140, 0.204]	0.114	<0.001	1021
200	Municipality	Theil	0.270	[0.234, 0.306]	0.193	<0.001	1021
300	Municipality	Theil	0.366	[0.325, 0.407]	0.256	<0.001	1021

Radius (m)	Scale	Index	β	95% CI	R^2	p	n
400	Municipality	Theil	0.431	[0.390, 0.473]	0.288	<0.001	1021
500	Municipality	Theil	0.480	[0.436, 0.524]	0.301	<0.001	1021
600	Municipality	Theil	0.514	[0.466, 0.562]	0.299	<0.001	1021
700	Municipality	Theil	0.538	[0.487, 0.589]	0.292	<0.001	1021
800	Municipality	Theil	0.552	[0.500, 0.605]	0.281	<0.001	1021
900	Municipality	Theil	0.554	[0.499, 0.609]	0.267	<0.001	1021
1000	Municipality	Theil	0.556	[0.500, 0.613]	0.257	<0.001	1021

Table S3. Canton-specific peak heat dates used for SCOPE model simulations. For each of the 22 Swiss cantons, the most extreme summer heat day in 2018 was identified as the date with the highest canton-averaged mean air temperature (Ta mean, ERA5 reanalysis at 100 m resolution). Hourly SCOPE simulations were run for each canton on its respective peak heat date to derive the Greening Cooling Services (GCoS) index. Appenzell Innerrhoden and Appenzell Ausserrhoden were merged for date detection due to their small size and geographic proximity.

Canton	Peak Heat Date	Ta mean (°C)
Appenzell*	05 Aug 2018	23.3
Bern	04 Aug 2018	25.4
Fribourg	03 Aug 2018	25.2
Geneva	05 Aug 2018	25.7
Glarus	05 Aug 2018	20.1
Graubünden	05 Aug 2018	17.4
Jura	04 Aug 2018	25.9
Lucerne	03 Aug 2018	25.8
Neuchâtel	03 Aug 2018	24.5
Nidwalden	05 Aug 2018	18.1
Obwalden	05 Aug 2018	18.9
Schaffhausen	03 Aug 2018	25.8
Schwyz	05 Aug 2018	23.7
Solothurn	04 Aug 2018	26.2
St. Gallen	05 Aug 2018	24.3
Thurgau	31 Jul 2018	27.1
Ticino	31 Jul 2018	25.1
Uri	05 Aug 2018	17.2
Valais	05 Aug 2018	20.9
Vaud	05 Aug 2018	24.8
Zug	05 Aug 2018	23.7
Zurich	03 Aug 2018	26.9

Table S4. Parameters of the exponential saturation model fitted to focal median cooling (GCoS) per sociodemographic group. a = asymptotic cooling plateau; b = rate constant (m^{-1}, reported $\times10^{-3}$); r_{50} = half-saturation distance (m); r_{95} = distance at which 95% of asymptotic cooling is reached (m); SE(r_{95}) = bootstrap standard error (200 within-group resamples); Δr_{95} = r_{95}(group) − r_{95}(reference); p = permutation test (500 permutations). The permutation test uses 500 iterations, which resolves p-values no smaller than 0.002; p-values are therefore reported at a resolution of 0.01. Reference groups are italicized.

Indicator	**Group**	**a**	**b ($\times10^{-3}$)**	**r_{50} (m)**	**r_{95} (m)**	**SE(r_{95})**	**Δr_{95} (m)**	**p-value**
Age group	*65-79 (ref.)*	*0.4906*	*39.5680*	*17.520*	*75.710*	*0.520*	—	—
Age group	0-25	0.4870	36.3100	19.090	82.510	0.540	6.790	<0.01
Age group	26-44	0.4723	33.7910	20.510	88.660	0.630	12.950	<0.01
Age group	45-64	0.4881	36.8250	18.820	81.350	0.570	5.640	<0.01
Age group	≥80	0.4839	39.9590	17.350	74.970	0.530	-0.740	0.336
Residence permit	*Swiss citizen (ref.)*	*0.4913*	*36.4890*	*19.000*	*82.100*	*0.580*	—	—
Residence permit	Long-term (B)	0.4596	33.4050	20.750	89.680	0.710	7.580	<0.01
Residence permit	Permanent (C)	0.4687	37.0980	18.680	80.750	0.540	-1.350	0.078
Residence permit	Short-term (L)	0.4431	17.9870	38.540	166.550	1.570	84.450	<0.01
Gender	*Male (ref.)*	*0.4840*	*35.5080*	*19.520*	*84.370*	*0.620*	—	—
Gender	Female	0.4834	36.8920	18.790	81.200	0.620	-3.160	<0.01
Civil status	*Married (ref.)*	*0.4900*	*36.8650*	*18.800*	*81.260*	*0.560*	—	—
Civil status	Divorced	0.4790	36.4330	19.030	82.230	0.590	0.960	0.226
Civil status	Single	0.4790	35.4970	19.530	84.390	0.580	3.130	<0.01
Civil status	Widowed	0.4833	37.9360	18.270	78.970	0.530	-2.290	<0.01
Socioeconomic position	*High (ref.)*	*0.5102*	*46.0500*	*15.050*	*65.050*	*0.390*	—	—
Socioeconomic position	Low	0.4633	30.0380	23.080	99.730	0.790	34.680	<0.01
Socioeconomic position	Lower-middle	0.4800	33.4400	20.730	89.580	0.620	24.530	<0.01
Socioeconomic position	Upper-middle	0.4919	38.1800	18.150	78.460	0.520	13.410	<0.01

Table S5. Multiple regression of individual-level cooling benefit (GCoS at 100 m focal radius) on five sociodemographic indicators simultaneously. Categorical variables are dummy-coded; reference groups are italicised. β = regression coefficient; SE = standard error; 95% CI = confidence interval; t = t-statistic; R^2 = coefficient of determination; F = F-statistic for overall model fit.

Indicator	Group	β	SE	95% CI [lower, upper]	t	p-value
Age group	*65–79 (ref.)*	*0.000*	—	—	—	—
Age group	0–25	0.018	0.000	[0.017, 0.018]	98.46	<0.001
Age group	26–44	-0.009	0.000	[-0.009, -0.008]	-57.34	<0.001
Age group	45–64	-0.001	0.000	[-0.001, -0.000]	-4.76	<0.001
Age group	≥80	-0.004	0.000	[-0.004, -0.003]	-16.05	<0.001
Residence permit	*Swiss citizen (ref.)*	*0.000*	—	—	—	—
Residence permit	Permanent (C)	-0.015	0.000	[-0.016, -0.015]	-136.01	<0.001
Residence permit	Long-term (B)	-0.028	0.000	[-0.028, -0.028]	-184.25	<0.001
Residence permit	Short-term (L)	-0.072	0.000	[-0.073, -0.071]	-176.79	<0.001
Gender	*Male (ref.)*	*0.000*	—	—	—	—
Gender	Female	0.000	0.000	[0.000, 0.001]	5.92	<0.001
Civil status	*Married (ref.)*	*0.000*	—	—	—	—
Civil status	Single	-0.024	0.000	[-0.024, -0.024]	-199.95	<0.001
Civil status	Divorced	-0.015	0.000	[-0.015, -0.014]	-93.53	<0.001
Civil status	Widowed	-0.010	0.000	[-0.011, -0.010]	-45.43	<0.001
Socioeconomic position	*High (ref.)*	*0.000*	—	—	—	—
Socioeconomic position	Upper-middle	-0.026	0.000	[-0.026, -0.026]	-209.40	<0.001
Socioeconomic position	Lower-middle	-0.042	0.000	[-0.043, -0.042]	-343.87	<0.001
Socioeconomic position	Low	-0.059	0.000	[-0.059, -0.059]	-498.82	<0.001

Model: n = 7,064,396; intercept = 0.4814; R^2 = 0.0594; adj. R^2 = 0.0594; $F(14, 7064381)$ = 31,860.4, $p < 0.001$

Table S6. Density-stratified comparison of cooling benefit (GCoS) at a focal radius of 100 m. Individuals are stratified into low, medium, and high population density tertiles. For each stratum, non-reference groups are compared to the reference group by bootstrap resampling (2,000 resamples). GCoS = Green Cooling Services index; IQR = interquartile range [25th, 75th percentile].

Density stratum	Indicator	Group	n	Median GCoS	IQR [P25, P75]	p-value
Low	*Age group*	*65–79 (ref.)*	*332,836*	*0.476*	*[0.402, 0.545]*	—
Low	Age group	0–25	657,125	0.474	[0.398, 0.546]	0.172
Low	Age group	26–44	533,326	0.462	[0.385, 0.537]	<0.001
Low	Age group	45–64	708,721	0.474	[0.399, 0.545]	0.117
Low	Age group	≥80	120,932	0.475	[0.400, 0.544]	0.287
Low	*Residence permit*	*Swiss citizen (ref.)*	*1,917,353*	*0.474*	*[0.401, 0.545]*	—
Low	Residence permit	Long-term (B)	126,656	0.458	[0.375, 0.540]	<0.001
Low	Residence permit	Permanent (C)	272,208	0.459	[0.380, 0.536]	<0.001
Low	Residence permit	Short-term (L)	20,966	0.416	[0.321, 0.504]	<0.001
Low	*Gender*	*Male (ref.)*	*1,180,549*	*0.471*	*[0.395, 0.544]*	—
Low	Gender	Female	1,178,430	0.472	[0.397, 0.544]	0.262
Low	*Civil status*	*Married (ref.)*	*1,070,650*	*0.474*	*[0.400, 0.545]*	—
Low	Civil status	Divorced	176,371	0.465	[0.389, 0.539]	<0.001
Low	Civil status	Single	1,002,381	0.470	[0.394, 0.544]	0.003
Low	Civil status	Widowed	109,404	0.467	[0.393, 0.538]	<0.001
Low	*Socioeconomic position*	*High (ref.)*	*546,051*	*0.518*	*[0.459, 0.577]*	—
Low	Socioeconomic position	Low	647,715	0.431	[0.355, 0.515]	<0.001
Low	Socioeconomic position	Lower-middle	606,049	0.452	[0.382, 0.526]	<0.001
Low	Socioeconomic position	Upper-middle	559,164	0.478	[0.412, 0.544]	<0.001
Medium	*Age group*	*65–79 (ref.)*	*309,940*	*0.431*	*[0.365, 0.491]*	—
Medium	Age group	0–25	626,726	0.427	[0.362, 0.489]	<0.001
Medium	Age group	26–44	628,255	0.419	[0.351, 0.483]	<0.001
Medium	Age group	45–64	637,551	0.427	[0.362, 0.487]	<0.001
Medium	Age group	≥80	134,263	0.430	[0.361, 0.490]	0.721
Medium	*Residence permit*	*Swiss citizen (ref.)*	*1,706,000*	*0.428*	*[0.363, 0.489]*	—
Medium	Residence permit	Long-term (B)	191,938	0.417	[0.345, 0.485]	<0.001
Medium	Residence permit	Permanent (C)	400,323	0.420	[0.353, 0.484]	<0.001
Medium	Residence permit	Short-term (L)	20,079	0.369	[0.290, 0.446]	<0.001
Medium	*Gender*	*Male (ref.)*	*1,152,632*	*0.424*	*[0.358, 0.486]*	—
Medium	Gender	Female	1,190,184	0.426	[0.361, 0.488]	0.042
Medium	*Civil status*	*Married (ref.)*	*974,460*	*0.428*	*[0.364, 0.489]*	—

Density stratum	Indicator	Group	n	Median GCoS	IQR [P25, P75]	p-value
Medium	Civil status	Divorced	207,474	0.424	[0.356, 0.486]	<0.001
Medium	Civil status	Single	1,040,331	0.423	[0.356, 0.486]	<0.001
Medium	Civil status	Widowed	120,232	0.424	[0.355, 0.485]	<0.001
Medium	*Socioeconomic position*	*High (ref.)*	*512,042*	*0.467*	*[0.415, 0.517]*	—
Medium	Socioeconomic position	Low	698,280	0.388	[0.322, 0.455]	<0.001
Medium	Socioeconomic position	Lower-middle	574,012	0.413	[0.350, 0.474]	<0.001
Medium	Socioeconomic position	Upper-middle	558,482	0.437	[0.378, 0.494]	<0.001
High	*Age group*	*65–79 (ref.)*	*256,100*	*0.412*	*[0.328, 0.483]*	—
High	Age group	0–25	630,011	0.406	[0.323, 0.477]	<0.001
High	Age group	26–44	765,188	0.384	[0.298, 0.461]	<0.001
High	Age group	45–64	572,809	0.400	[0.314, 0.474]	<0.001
High	Age group	≥80	116,138	0.410	[0.324, 0.483]	<0.001
High	*Residence permit*	*Swiss citizen (ref.)*	*1,458,917*	*0.405*	*[0.322, 0.476]*	—
High	Residence permit	Long-term (B)	294,414	0.376	[0.287, 0.455]	<0.001
High	Residence permit	Permanent (C)	514,050	0.398	[0.314, 0.472]	<0.001
High	Residence permit	Short-term (L)	33,845	0.302	[0.189, 0.397]	<0.001
High	*Gender*	*Male (ref.)*	*1,153,425*	*0.396*	*[0.310, 0.470]*	—
High	Gender	Female	1,192,951	0.401	[0.316, 0.474]	<0.001
High	*Civil status*	*Married (ref.)*	*852,843*	*0.409*	*[0.326, 0.479]*	—
High	Civil status	Divorced	218,578	0.398	[0.310, 0.474]	<0.001
High	Civil status	Single	1,172,003	0.390	[0.303, 0.465]	<0.001
High	Civil status	Widowed	101,873	0.407	[0.322, 0.480]	0.788
High	*Socioeconomic position*	*High (ref.)*	*409,614*	*0.408*	*[0.325, 0.481]*	—
High	Socioeconomic position	Low	841,383	0.387	[0.302, 0.463]	<0.001
High	Socioeconomic position	Lower-middle	571,118	0.400	[0.312, 0.474]	<0.001
High	Socioeconomic position	Upper-middle	524,261	0.407	[0.323, 0.477]	0.139